Full Papers
doi.org/10.1002/ejic.202000942

Chemistry Europe
European Chemical Societies Publishing

N-Heterocyclic Silylene Main Group Element Chemistry: Adduct Formation, Insertion into E–X Bonds and Cyclization of Organoazides

Mirjam J. Krahfuss[a] and Udo Radius*[a]

Investigations concerning the reactivity of the *N*-heterocyclic silylene $Dipp_2NHSi$ (**1**, 1,3-bis(2,6-di*iso*propylphenyl)-1,3-diaza-2-silacyclopent-4-en-2-ylidene) towards selected alanes and boranes, elemental halides X_2 (X = Br, I), selected halide containing substrates such as tin chlorides and halocarbons, as well as organoazides are presented. The NHSi adducts $Dipp_2NHSi{\cdot}AlI_3$ (**2**), $Dipp_2NHSi{\cdot}Al(C_6F_5)_3$ (**3**), and $Dipp_2NHSi{\cdot}B(C_6F_5)_3$ (**4**) were formed by the reaction of $Dipp_2NHSi$ with the corresponding *Lewis* acids AlI_3, $Al(C_6F_5)_3$ and $B(C_6F_5)_3$. Adducts **3** and **4** were tested with respect to their ability to activate small organic molecules, but no frustrated *Lewis* pair reactivity was observed. Reactions of $Dipp_2NHSi$ with Br_2, I_2, Ph_2SnCl_2 and Me_3SnCl led to formation of $Dipp_2NHSiBr_2$ (**5**), $Dipp_2NHSiI_2$ (**6**), $Dipp_2NHSiCl_2$ (**7**) and $\{(Me_3Sn)N(Dipp)CH\}_2$ (**8**), respectively. The reaction with the halocarbons methyl iodide, benzyl chloride, and benzyl bromide afforded the insertion products $Dipp_2NHSi(I)(CH_3)$ (**9**), $Dipp_2NHSi(Cl)(CH_2Ph)$ (**10**) and $Dipp_2NHSi(Br)(CH_2Ph)$ (**11**). Reaction of $Dipp_2NHSi$ with the organoazides Ad-N_3 (Ad = adamantyl) and TMS-N_3 (TMS = trimethylsilyl) led to the formation of 1-$Dipp_2NHSi$-2,5-bis(adamantyl)-tetrazoline (**12**) and bis(trimethylsilyl)amido azido silane (**13**), respectively. For 2,6-(diphenyl) phenyl-N_3 C–H activation occurs and a cyclosilamine **14** was isolated.

Introduction

Since their first synthesis in 1994,[1] *N*-heterocyclic silylenes (NHSis) were established as useful ligands for transition metal complexes.[2] In the following decades, the properties of *Arduengo*-type NHCs[3] and also of NHSis[4] towards main group element compounds were examined. Although NHCs and NHSis are in principle isostructural, the replacement of the carbene carbon atom with a silicon atom has a significant impact on the electronic features and thus on the reactivity of NHSis compared to NHCs. We have shown earlier that the frontier molecular orbitals of NHSi and NHCs significantly differ, as shown in Figure 1 for some commonly used examples of this class of compounds, e.g. $Dipp_2NHSi$ **1** (1,3-bis(2,6-di*iso*propylphenyl)-1,3-diaza-2-silacyclopent-4-ene-2-ylidene) and the NHC analogue $Dipp_2Im$ (1,3-bis(2,6-di*iso*propylphenyl)-imidazolin-2-ylidene).[5]

The frontier orbitals of $Dipp_2NHSi$ (**1**) and $Dipp_2Im$ differ according to DFT calculations (def2-TZVPP/B3-LYP-D3(BJ)). The HOMO of the carbene $Dipp_2Im$ at −5.94 eV has σ-symmetry with respect to the imidazole ring plane and the LUMO at 0.64 eV is of π-symmetry, which leads to an energy gap of 6.58 eV. For the silylene $Dipp_2NHSi$ the orbital order of HOMO and HOMO-1 is reversed, which leads to a HOMO of π-symmetry at −5.48 eV and a HOMO-1 at −6.48 eV of σ-symmetry. The LUMO of $Dipp_2NHSi$, which is of π-character, lies at −0.87 eV, much lower than the LUMO of $Dipp_2Im$, and leads to an energy gap of 4.61 eV. Another commonly used important class of ligands in both transition metal and main group element chemistry are cyclic (alkyl)(amino)carbenes (cAAC),[6] which have a rather small HOMO-LUMO gap compared to NHCs and NHSis, e.g. 3.1 eV for $cAAC^{Me}$ with a HOMO of σ-symmetry at −4.43 eV and the LUMO of π-symmetry at −1.33 eV. We have demonstrated earlier that these differences in the electronic features of NHSis (compared to NHCs) lead to interesting differences in the transition metal coordination chemistry of NHSis.[5] In particular, the low lying π-acceptor orbital seems to be responsible for silylenes being much better bridging ligands compared to NHCs. However, these different electronic features should be also present in the coordination chemistry/adduct formation with main group element compounds or in main group element chemistry in general. We thus were interested to investigate and compare the reactivity of NHSi **1** with those of NHCs and cAACs. Herein, we want to report on some reactions of $Dipp_2NHSi$ with main group element compounds such as X_2 (X = Br, I), selected halide containing substrates, selected alanes and boranes as well as selected azides.

Results and Discussion

N-heterocyclic silylenes can act as *Lewis* acids and *Lewis* bases simultaneously and thus, reacting $Dipp_2NHSi$ (**1**) with *Lewis*

[a] *M. J. Krahfuss, Prof. Dr. U. Radius*
Institut für Anorganische Chemie
Julius-Maximilians-Universität Würzburg
Am Hubland, 97074 Würzburg, Germany
E-mail: u.radius@uni-wuerzburg.de
http://www.ak-radius.de

Supporting information for this article is available on the WWW under https://doi.org/10.1002/ejic.202000942

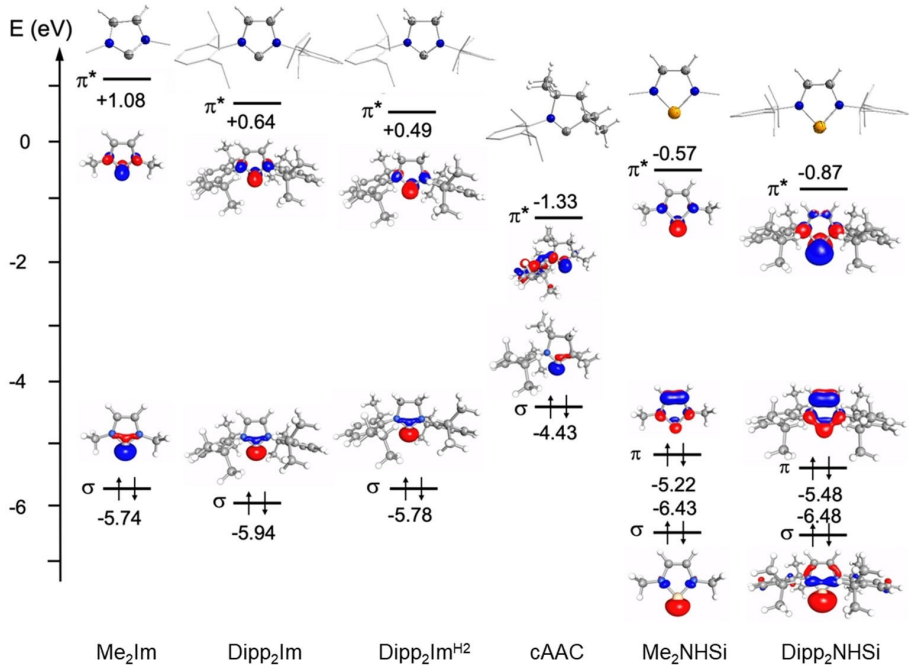

Figure 1. Important frontier orbitals of the NHSis Me_2NHSi and $Dipp_2$NHSi with respect to those of commonly used NHCs Me_2Im, $Dipp_2$Im, $Dipp_2Im^{H2}$, and $cAAC^{Me}$. Energies were calculated at the DFT/def2-TZVPP/B3-LYP–D3(BJ) level of theory and orbital plots are drawn at the 0.1 isosurface.

acidic alanes or boranes should lead to the formation of classical or frustrated *Lewis* acid/base pairs. As silylene **1** is sterically demanding,[5] using an alane or borane with steric bulk could favor the formation of frustrated *Lewis* pairs (FLP). For phosphines and *N*-heterocyclic carbenes, several known FLP compounds containing congested boranes as *Lewis* acids have been synthesized and their reactivity towards small molecules such as dihydrogen,[7] THF,[7d,8] C–C multiple bonds,[9] carbon dioxide[10] and singlet dioxygen[11] has been studied.

Alane-based adducts of NHCs have also been investigated, e.g. Dagorne and co-workers reported the activation of dihydrogen by tBu$_2$Im·Al(iBu)$_3$ giving tBu$_2$Im(H)$_2$ (tBu$_2$Im = 1,3-di-*tert*-butyl-imidazolin-2-ylidene).[12] Keeping in mind that phosphines and *N*-heterocyclic silylenes have been shown to possess similar characteristics with regard to transition metal chemistry,[5] we were interested in the *Lewis* base properties of $Dipp_2$NHSi (**1**) with respect to typical group 13 *Lewis* acids and investigated in the beginning different simple aluminum halides. With $AlCl_3$, no reaction or formation of an adduct was observed. Interestingly, the reaction of silylene **1** with one equivalent of aluminum triiodide in toluene led to the clean formation of $Dipp_2$NHSi·AlI_3 (**2**) as an off-white solid in very good yields (87% isolated yield, Scheme 1). In the ^{29}Si NMR spectrum of **2**, a resonance at 42.8 ppm was detected and the aluminum atom gave rise to a signal at 40.1 ppm in the ^{27}Al NMR spectrum.[6,13] One set of signals was observed for the NHSi group in the ^{1}H NMR spectrum, which indicated the formation of a symmetric compound. Thus, no insertion into the Al–I bond but the formation of the NHSi aluminum adduct $Dipp_2$NHSi·AlI_3 (**2**, Scheme 1) occurred. The characteristic septet

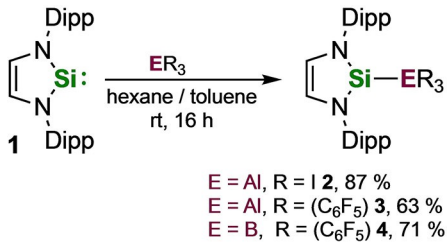

Scheme 1. Synthesis of the NHSi adducts $Dipp_2$NHSi·AlI_3 (**2**), $Dipp_2$NHSi·Al(C_6F_5)$_3$ (**3**) and $Dipp_2$NHSi·B(C_6F_5)$_3$ (**4**).

of the methine protons was shifted towards higher fields to 3.08 ppm (**1**: 3.25 ppm).

Metzler and Denk reported previously the silylene borane adduct tBu$_2$NHSi·B(C_6F_5)$_3$ (tBu$_2$NHSi: 1,3-*tert*-butyl-1,3-diaza-2-silacyclopent-4-en-2-ylidene) which slowly undergoes a rearrangement with insertion of the silylene silicon atom into one of the B–C bonds to give tBu$_2$NHSi(C_6F_5)-B(C_6F_5)$_2$.[14] The reaction of $Dipp_2$NHSi with the perfluorinated alane Al(C_6F_5)$_3$ and borane B(C_6F_5)$_3$ in toluene/hexane mixtures provided the adducts $Dipp_2$NHSi·Al(C_6F_5)$_3$ (**3** 63%) and $Dipp_2$NHSi·B(C_6F_5)$_3$ (**4** 71%) in good yields. In the ^{29}Si NMR spectra, the NHSi silicon atoms were found to be slightly shifted towards higher fields at 74.0 ppm (**3**) and 72.2 ppm (**4**) and in the ^{1}H NMR spectra of **3** and **4** one set of resonances was observed for the NHSi ligand, which excluded the formation of rearrangement products. The boron atom of adduct **4** was detected at −19.9 ppm in the ^{11}B NMR spectrum, at higher fields compared to the adduct tBu$_2$NHSi·B(C_6F_5)$_3$ reported previously (−14.3 ppm).[14] The aluminum atom of **3** was not observed in the ^{27}Al NMR spectrum.

However, for both compounds, one set of resonances was detected for the fluorine substituents of the perfluorophenyl groups at −123.0, −150.7, and −160.5 ppm (**3**) and at −129.0, −155.9, and −162.2 ppm (**4**), respectively. For both adducts **3** and **4**, no rearrangement products were detected even after prolonged storage of these compounds in solvents such as benzene, toluene, or hexane. Single crystals of **4** suitable for X-ray diffraction were grown from a saturated hexane solution of **4** at −30 °C (Figure 2).

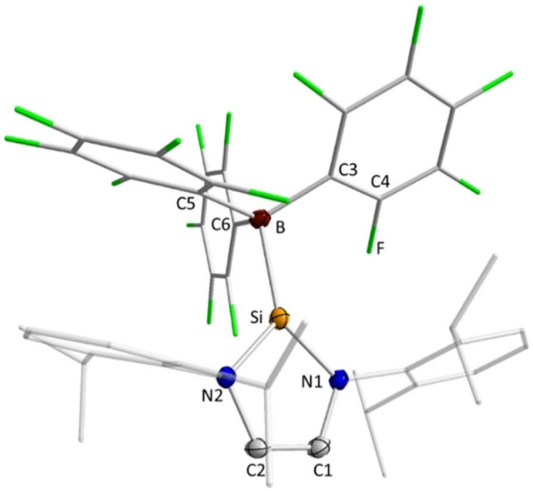

Figure 2. Molecular structure of $Dipp_2NHSi{\cdot}B(C_6F_5)_3$ (**4**) in the solid state (ellipsoids drawn at the 50 % probability level; hydrogen atoms omitted for clarity). Selected bond lengths [Å] and angles [°] of **4**: Si-N1 1.6993(18), Si-N2 1.7085(17), Si-B 2.077(2), N1–C1 1.407(3), N2–C2 1.410(3), C1–C2 1.328(3), B–C3 1.634(3), B–C5 1.622(3), B–C6 1.627(3), C4–F 1.345(3), N1–Si-N2 92.85(9), C3–B–Si 109.15(15), C5–B–Si 100.66(13), C6–B–Si 108.59(15), (N–C1–C2–N2) / (N1–Si-N2) 3.41(8).

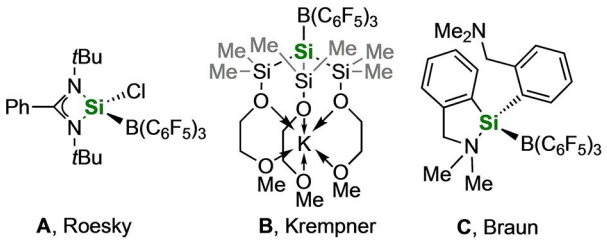

Figure 3. Examples of silicon-containing boron adducts with a silicon–boron bond.

Following the synthesis and characterization of the perfluorinated adducts $Dipp_2NHSi{\cdot}Al(C_6F_5)_3$ (**3**) and $Dipp_2NHSi{\cdot}B(C_6F_5)_3$ (**4**), we opted to investigate whether compounds **3** and **4** react as compounds with frustrated *Lewis* pairs with selected substrates. To test the ability to activate small molecules, the adducts **3** and **4** were dissolved in C_6D_6 in a Young-tap NMR tube, the respective substrate was added, and the reaction progress was monitored *via* ^1H and ^{29}Si NMR measurements after 16 h. Dihydrogen activation by a FLP was first reported by Stephan and co-workers who used a phosphine borane to heterolytically split H_2,[7d] and Tamm and co-workers utilized the NHC borane adduct $tBu_2Im{\cdot}B(C_6F_5)_3$ for cleavage of the H–H bond.[7b] However, using the NHSi borane adduct **4** no reaction was observed upon treatment with dihydrogen. Furthermore, white phosphorus and diphenylacetylene were used as substrates but only starting material was identified in the NMR spectra. In the case of **3**, carbon monoxide (see Figure 4) and phenylacetylene were used and no reaction was observed after 16 h at room temperature. As conclusion, in contrast to the NHC adducts of alanes and boranes, which readily activate

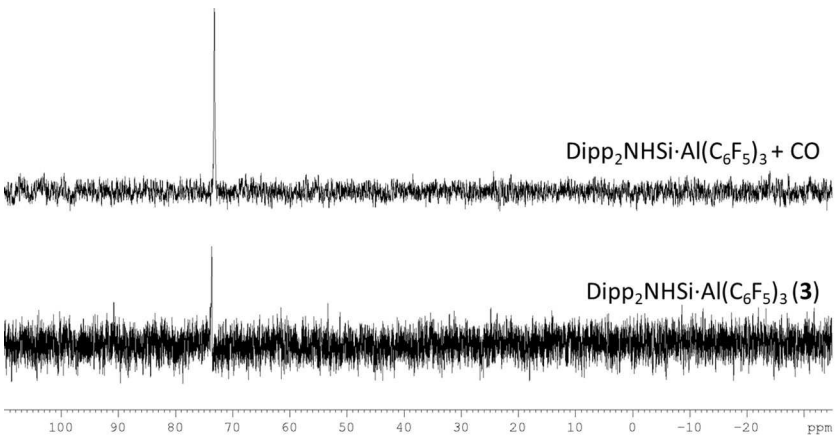

Figure 4. ^{29}Si NMR spectra of $Dipp_2NHSi{\cdot}Al(C_6F_5)_3$ (**3**) (bottom) and of the reaction of $Dipp_2NHSi{\cdot}Al(C_6F_5)_3$ (**3**) with carbon monoxide in C_6D_6 after 16 h at room temperature (top).

small organic molecules, the silylene adducts **3** and **4** do not show any FLP reactivity.

We were also interested in the reactivity of the NHSi towards some simple inorganic and organic molecules.

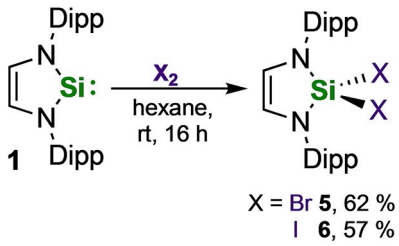

Scheme 2. Reaction of $Dipp_2NHSi$ with Br_2 and I_2.

Table 1. ^1H and ^{29}Si NMR shifts of selected resonances of the silanes $Dipp_2NHSiCl_2$ **7**,[18] $Dipp_2NHSiBr_2$ **5**, $Dipp_2NHSiI_2$ **6**, $Dipp_2NHSi(I)(CH_3)$ **9**, $Dipp_2NHSi(Cl)(CH_2Ph)$ **10** and $Dipp_2NHSi(Br)(CH_2Ph)$ **11**.

Compound	δ ($CH(CH_3)_2$) [ppm]	δ ($CHCH$) [ppm]	δ (Si) [ppm]
$Dipp_2NHSiCl_2$ **7**[18]	3.52	5.82	−38.1
$Dipp_2NHSiBr_2$ **5**	3.71	5.74	−59.3
$Dipp_2NHSiI_2$ **6**	3.76	5.77	−134.5
$Dipp_2NHSi(I)(CH_3)$ **9**	3.37, 4.04	5.75	−30.4
$Dipp_2NHSi(Cl)(CH_2Ph)$ **10**	3.51, 3.92	5.74	−19.4
$Dipp_2NHSi(Br)(CH_2Ph)$ **11**	3.52, 3.98	5.76	−20.9

$Dipp_2NHSi$ reacted cleanly with Br_2 or I_2 in non-polar solvents like toluene, benzene, or hexane to give the oxidized compounds $Dipp_2NHSiBr_2$ (**5**) and $Dipp_2NHSiI_2$ (**6**) which can be isolated from hexane as pale-yellow solids in moderate yields (**5**: 62%, **6**: 57%, Scheme 2).

Interestingly, compounds **5** and **6** are highly sensitive to traces of air and moisture, but well stable in solution and in the solid if kept under an argon atmosphere. The oxidation of the silylene $Dipp_2NHSi$ leads to characteristic shifts in the ^1H and ^{29}Si NMR spectra. ^1H and ^{29}Si NMR shifts of important resonances of **5–7** are summarized in Table 1. The methine protons of **5** and **6** give rise to a septet at 3.71 ppm (**5**) and 3.76 ppm (**6**) and thus show a significant low-field shift compared to the free silylene (3.25 ppm). The CH groups of the backbone also experience a noticeable shift to higher fields from 6.46 ppm ($Dipp_2NHSi$) to 5.74 ppm (**5**) and 5.77 ppm (**6**). In the ^{29}Si NMR spectrum, a clear tendency was observed going from $Dipp_2NHSiCl_2$ (**7**: −38.6 ppm, see below)[18] to $Dipp_2NHSiBr_2$ (**5**: −59.3 ppm) to $Dipp_2NHSiI_2$ (**6**: −134.5 ppm). Single crystals of **5** and **6** suitable for X-ray diffraction were grown from a saturated hexane solution of **5** at −30 °C and by slow evaporation of a saturated hexane solution of **6** at room temperature. The molecular structures of these compounds in the solid state are shown in Figure 5.

$Dipp_2NHSiBr_2$ (**5**) and $Dipp_2NHSiI_2$ (**6**) crystallize in the orthorhombic space group Pnma and the molecular structures reveal a tetrahedrally coordinated silicon atom. The NHSi ring is

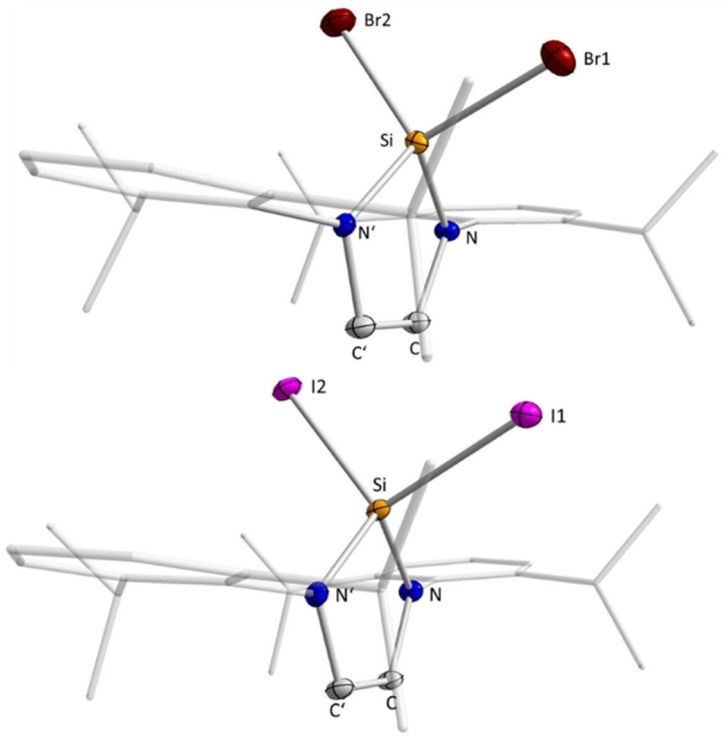

Figure 5. Molecular structures of $Dipp_2NHSiBr_2$ (**5**) (top) and $Dipp_2NHSiI_2$ (**6**) (bottom) in the solid state (ellipsoids drawn at the 50% probability level; hydrogen atoms omitted for clarity). Selected bond lengths [Å] and angles [°] of **5**: Si–N 1.7059(19), Si–Br1 2.2239(10), Si–Br2 2.1866(9), N–C 1.417(3), C–C′ 1.328(5), N–Si-N′ 93.86(13), Br1–Si–Br2 102.18(4), Br1–Si–N 114.62(7), Br2–Si–N′ 116.17(7), (N–C–C′–N′) / (N–Si–N′) 6.66(13); selected bond lengths [Å] and angles [°] of **6**: Si–N 1.711(2), Si–I1 2.4861(10), Si–I2 2.4240(9), N–C 1.420(3), C–C′ 1.331(6), N–Si-N′ 93.80(15), I1–Si–I2 102.99(4), I1–Si–N 113.98(8), I2–Si–N′ 116.36(8), (N–C–C′–N′) / (N–Si–N′) 8.0(2).

almost planar, with the silicon atoms slightly bent out of the plane of the nitrogen and the backbone carbon atoms (**5**: 6.66(13)°, **6**: 8.0(2)°). Interestingly, the silicon-halide bond lengths of 2.2239(10) Å (Si–Br1) and 2.1866(9) Å (Si–Br2) (**5**) and 2.4861(10) Å (Si–I1) and 2.4240(9) Å (Si–I2) (**6**) differ, respectively. All other bond lengths and angles are unremarkable and in accordance with the molecular structure reported for $Dipp_2NHSiCl_2$ (**7**).[22]

As only little is known about the reactivity of $Dipp_2NHSi$ (**1**) towards main group element halide compounds, we reacted **1** with some secondary and tertiary tin chlorides (Scheme 3).

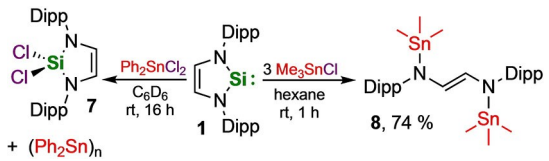

Scheme 3. Reaction of $Dipp_2NHSi$ (**1**) with the halostannanes Ph_2SnCl_2 and Me_3SnCl.

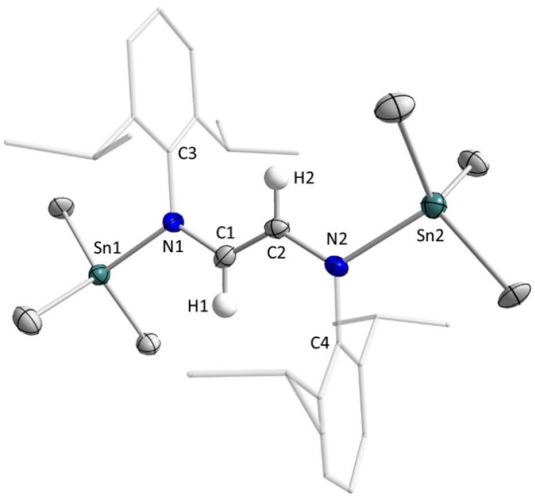

Figure 6. Molecular structure of $\{(Me_3Sn)N(Dipp)CH\}_2$ (**8**) in the solid state (ellipsoids drawn at the 50% probability level; hydrogen atoms except at the carbon atoms C1 and C2 omitted for clarity). Selected bond lengths [Å] and angles [°] of **8**: Sn1–N1 2.074(5), N1–C1 1.407(8), C1–C2 1.333(10), C2–N2 1.402(8), N2–Sn2 2.079(5), Sn1–N1–C1 118.9(4), Sn1–N1–C3 121.7(4). C3–N1–C1 117.7(5), N1–C1–C2 126.5(6), C1–C2–N2 126.0(6), C2–N2–Sn2 119.3(4), C2–N2–C4 118.5(5), C4–N2–Sn2 121.0(4), distance Sn1 from (N1–C1–C2–N2): 0.3497(4), distance Sn2 from (N1–C1–C2–N2): 0.3615(4).

The reaction of $Dipp_2NHSi$ (**1**) with Ph_2SnCl_2 afforded the dichlorosilane $Dipp_2NHSiCl_2$ (**7**, Scheme 3, left), which was characterized by NMR spectroscopy (see Experimental Part). The silylene acts here as a reducing reagent for the dichlorostannane and the thermodynamic driving force can easily be explained by the different bond enthalpies.[19] Monitoring the reaction in a Young-tap NMR tube, we observed several signals in the range between −198.6 and −218.6 ppm in the ^{119}Sn spectrum, which can be assigned to cyclic poly(diphenylstannanes) like $(Ph_2Sn)_6$.[20] However, if $Dipp_2NHSi$ was reacted with Me_3SnCl in organic solvents such as hexane, benzene, toluene, or THF cleavage of the NHSi ring with the formation of the distannyl diazabutene **8** was observed (Scheme 3, right). The silicon atom of the silylene reacts with a third equivalent of Me_3SnCl to presumably afford a stannyl silane. The ring-opening of **1** in the reaction with three equivalents of Me_3SnCl occurs in solution spontaneously and, interestingly, also solvent-free in the solid state within a few minutes as observed by the change of color. Compound **8** was isolated from hexane in yields of 74% and was characterized by NMR spectroscopy, elemental analysis and X-ray diffraction (Figure 6). The stannyl substituents give rise to a signal at −118.0 ppm in the ^{119}Sn NMR spectrum and the carbon atoms of the diazabutene backbone were observed at 123.8 ppm in the $^{13}C\{^1H\}$ NMR spectrum. Monitoring the reaction in a Young-tap NMR tube leads to the observation of a second reaction product giving a resonance at −15.6 ppm in the ^{29}Si NMR spectrum and a resonance at 57.9 ppm in the ^{119}Sn NMR spectrum.

The diazabutene moiety N1–C1(H1)–C2(H2)–N2 of **8** is planar and the tin atoms are only very slightly bend out of the plane (Sn1 0.3497(4) Å, Sn2 0.3615(4) Å). The sum of angles at the planar nitrogen atoms are 358.3° (N1) and 358.8° (N2) and the C1–C2 bond between the carbon atoms of the diazabutene backbone of 1.333(10) Å lies in the range of a C=C double bond (1.34 Å).[21]

Whereas NHSi insertion into main group element halide bonds was observed rather often, the complete halide transfer to the NHSi with reduction of the substrate has not been exploited thoroughly in experimental chemistry yet. For the former, Denk and co-workers reported previously for example the reaction of tBu_2NHSi with tin dichloride in a 3:2 ratio to yield the tris(chlorosilyl)stannane **D** (Figure 7, left), which was formed by the insertion of the silylene silicon atoms into the tin-chloride bonds, and stochiometric amounts of elemental tin (Figure 7, left).[22] Braunschweig and co-workers demonstrated

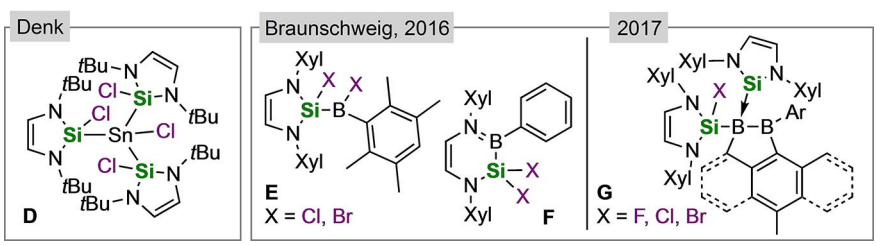

Figure 7. The reaction of *N*-heterocyclic silylenes with tin dichloride, aryl dihaloboranes, and aryl dihalodiboranes(4).

that the reaction of Xyl_2NHSi with aryl dihaloboranes led to the insertion of the silylene silicon atom into the boron–halogen bond to yield silyl boranes **E** for R = Duryl and NHSi-ring expanded products **F** for R = Ph (Figure 7, middle).[23] When aryl dihalodiboranes(4) were used as reactants, diboranes **G** featuring one halosilyl and one silylene ligand were obtained (Figure 7, right).

Some examples of reactions of *N*-heterocyclic silylenes with halocarbons have been published so far, but the majority of them were performed using the *tert*-butyl silylene tBu_2NHSi.[4c,24] For $Dipp_2NHSi$, the reaction of **1** with the halocarbons methyl iodide, benzyl chloride, and benzyl bromide led to the insertion of the silicon atom into the C–X bond to give $Dipp_2NHSi(I)(CH_3)$ (**9**), $Dipp_2NHSi(Cl)(CH_2Ph)$ (**10**) and $Dipp_2NHSi(Br)(CH_2Ph)$ (**11**) (Scheme 4). Thus, insertion seems to be favored over the formation of $Dipp_2NHSiX_2$ (X=Cl, Br, I) and even the usage of an excess of the benzyl halides (up to three equivalents) or methyl iodide (five-fold excess) led to the formation of **9–11**. The compounds **9–11** were isolated from hexane in good yields (**9** 81 %, **10** 82 %, **11** 75 %) as analytically pure, yellow (**9**, **10**) or colorless (**11**) solids. These compounds are well soluble in common halide-free organic solvents such as Et_2O, THF, benzene or toluene and sensitive to air and moisture.

For compounds **9–11** a doubled set of signals for the Dipp substituents at the nitrogen atoms were observed in the ^1H and ^{13}C NMR spectra due to the two different substituents at the silicon atoms. For example, the ^1H NMR spectra of **9–11** reveal septets for the methine protons at 3.37 and 4.04 ppm (**9**), 3.51 and 3.92 ppm (**10**), and 3.52 and 3.98 ppm (**11**), while the protons of the backbone are single resonances at 5.75 ppm (**9**), 5.74 ppm (**10**) and 5.76 ppm (**11**). In the ^{29}Si NMR spectrum, the singlets of the silicon atom are high field shifted (**9**: −30.3 ppm, **10**: −19.4 ppm, **11**: −20.9 ppm) compared to $Dipp_2NHSi$. Important ^1H and ^{29}Si NMR shifts of resonances of **9–11** are summarized in Table 1.

Single crystals of **9** suitable for X-ray diffraction were grown from a saturated hexane solution at −30 °C and crystals of **11** were obtained by vapor diffusion of hexane into a saturated solution of **11** in 1,2-difluorobenzene. The molecular structures of **9** and **11** in the solid state are shown in Figure 8. The silanes **9** and **11** crystallize in the orthorhombic space groups Pnma and $P2_12_12_1$, respectively, and have an almost planar NHSi ring with the silicon atom being bent out of the plane by 10.68(13)° (**9**) and 10.4(3)° (**11**). The tetrahedral coordination at the silicon atoms is significantly distorted as is shown by the angles

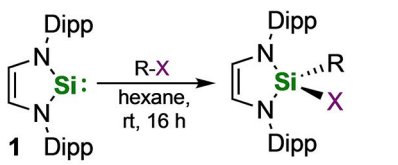

R = CH_3, X = I **9**, 81 %
R = CH_2Ph, X = Cl **10**, 82 %
R = CH_2Ph, X = Br **11**, 75 %

Scheme 4. Synthesis of $Dipp_2NHSi(I)(CH_3)$ (**9**), $Dipp_2NHSi(Cl)(CH_2Ph)$ (**10**) and $Dipp_2NHSi(Br)(CH_2Ph)$ (**11**).

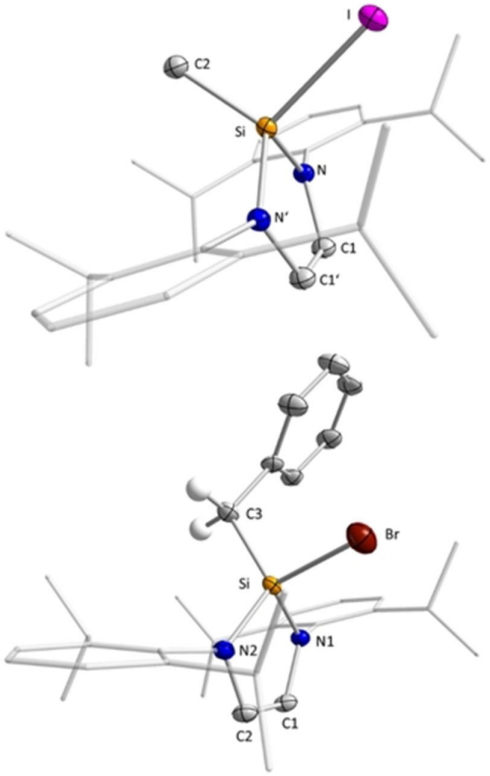

Figure 8. Molecular structures of $Dipp_2NHSi(I)(CH_3)$ (**9**) (top) and $Dipp_2NHSi(Br)(CH_2Ph)$ (**11**) (bottom) in the solid state (ellipsoids drawn at the 50 % probability level; hydrogen atoms omitted for clarity). Selected bond lengths [Å] and angles [°] of **9**: Si–N 1.7202(14), Si–I 2.5220(6), Si–C2 1.858(2), N–C1 1.420(2), C1–C1′ 1.338(4), N–Si–N′ 92.69(10), I–Si–C2 102.86(8), I–Si–N 111.98(5), C2–Si–N′ 118.82(7), I–Si–N 111.98(5), C2–Si–N 118.82(7), (N–C1–C1′–N′) / (N–Si-N′) 10.68(13). Selected bond lengths [Å] and angles [°] of **11**: Si–N1 1.722(4), Si–N2 1.723(4), Si–C3 1.874(5), N–C1 1.423(6), C1–C2 1.323(7), C2–N2 1.416(6), N1–Si–N2 93.08(19), Br–Si–C3 104.38(15), Br–Si–N1 112.92(14), Br–Si–N2 111.14(15), C3–Si–N1 116.5(2), C3–Si–N2 119.0(2), (N1–C1–C2–N2) / (N1–Si–N2) 10.4(3).

N–Si–N of 92.69(10)° (**9**) and 93.08(19)° (**11**), but also by the angles of the halogen substituents (**9**: 111.98(5)°, **11**: 112.92(14)°) and the methyl/benzyl substituent to the plane generated by the five-membered ring (**9**: 118.82(7)°, **11**: 119.0(2)°).

Whereas C–Cl, C–Br, and C–I bonds are readily activated by $Dipp_2NHSi$ (**1**), all of our attempts to activate the C–F bond of polyfluoroaryls using **1** were unsuccessful, and only starting material was observed even after prolonged heating. For NHCs and cAACs, it has been demonstrated previously that these carbenes activate and insert into the C–F bonds of perfluorinated arenes[25] or perfluorinated alkenes.[26] In these reactions, two different products have been observed: (i) insertion products into the carbon-fluorine bond[25c,e–g,26] and (ii) products from heterolytic C–F bond cleavage, especially in the presence of fluoride acceptors, which leads to arylation of the NHC and formation of a salt of the type $[R_2Im\text{-}aryl^F][X]$ (X=F^-, HF_2^-, BF_4^-).[25a,b,d] Arduengo and co-workers reported at the end of the 1990s on C–Cl and C–I activation of chloro and iodo alkanes.[27] If the backbone methylated carbene Me_2Im^{Me} (1,3,4,5-tetrameth-

ylimidazolin-2-ylidene) was reacted with $CHClX_2$ (X=Cl, F) the corresponding imidazolium salts $[Me_2Im^{Me}\text{-}CHX_2][Cl]$ were formed.[27a] The saturated carbene Mes_2Im^{H2} (1,3-dimesitylimidazolidin-2-ylidene) reacted with CH_2Cl_2, CH_3I or CCl_4 to give the imidazolium salts $[Mes_2Im^{H2}\text{-}CH_2Cl][Cl]$, $[Mes_2Im^{H2}\text{-}CH_3][I]$ and $[Mes_2Im^{H2}\text{-}Cl][Cl_3]$ as intermediates, which subsequently were transferred to the *N*-heterocyclic olefins (NHOs) $Mes_2Im^{H2}=CHCl$, $Mes_2Im^{H2}=CH_2$ and $Mes_2Im^{H2}=CCl_2$, respectively.[27b] Treatment of the unsaturated analog Mes_2Im (1,3-dimesitylimidazolin-2-ylidene) with carbon tetrachloride, on the other hand, led to the substitution of the hydrogen atoms of the backbone of the NHC to give Mes_2Im^{Cl2} (1,3-dimesityl-4,5-dichloro-imidazolin-2-ylidene), which then reacts with CCl_4 to yield the salt $[Mes_2Im^{Cl2}\text{-}Cl][Cl]$ and the NHO $Mes_2Im^{Cl2}=CCl_2$.[27b]

For *West/Denk*-type NHSis, a variety of examples are available for reactions with organyl chlorides,[4c,24a,28] bromides[24a] and iodides,[28a,29] but no studies on the reaction of NHSis with fluorocarbons have been presented so far. Roesky and Sen reported on the C–F activation of aryl fluorides using three coordinate silylenes $PhC(NtBu)_2SiR$ ($R=N(SiMe_3)_2$, Cl)[30] or the cyclic silylene $CH\{(CH{=}CH_2)(CMe)\text{-}(Dipp)_2\}Si$,[31] which gave the insertion products $PhC(NtBu)_2Si(R)(F)(aryl^F)$ and $CH[\{(CH{=}CH_2)(CMe)\text{-}(Dipp)_2\}Si(F)(aryl^F)$. As observed for transition metal chemistry, most studies for NHSis have been conducted with the *tert*-butyl substituted NHSis tBu_2NHSi and tBu_2NHSi^{H2} (1,3-di-*tert*-butyl-1,3-diaza-2-silacyclopent-2-ylidene) as well as a benzannulated NHSi.[29] These investigations reveal that tBu_2NHSi and tBu_2NHSi^{H2} react with a variety of chloro- or bromocarbons to yield to the monosilanes **H**, disilanes **I** or mixtures of both, depending on the halocarbon and the stoichiometric ratio used (Figure 9, top left).[4c,24a] Holl and co-workers reacted tBu_2NHSi with phenyl iodide to obtain $tBu_2NHSi(I)(Ph)$, and subsequent addition of *N*-methyl piperidine led to the isolation of $tBu_2NHSi(I)(Py^{Me})$ via a C–H activation in *ortho*-position of the piperidine nitrogen atom.[24b] Furthermore, it was shown that two molecules of the benzannulated, CH_2tBu substituted silylene $(tBuCH_2)_2NHSi^{benz}$ insert into the C–Cl (C–Br) bonds of dichloromethane or dibromo methane, respectively, to give the methylene bridged disilane **J** (Figure 9, bottom left).[29] Dinuclear compounds **K** were also observed by Kira and co-workers who reported studies on the reactivity of an isolable dialkylsilylene (Figure 9, right) towards halocarbons.[28] The reaction of the dialkyl silylene with $CHCl_3$ and CCl_4 led to the exclusive formation of the oxidized silylene **L**, whereas the carbon-iodine insertion product was observed upon reaction with methyl iodide.[28a] For the aryl-substituted stable NHSis Xyl_2NHSi, Mes_2NHSi, and $Dipp_2NHSi$, no studies were reported so far concerning the reactivity towards halocarbons.

To further investigate the differences and similarities between NHCs and NHSis, we reacted $Dipp_2NHSi$ with azides to compare the results obtained to the products observed for the reaction with NHCs. The first silatetrazoline was synthesized in 1978 *via* the oxidation of a silylated lithium hydrazide with tosyl azide.[32] In 1997, West and colleagues reported the synthesis and structural studies on cyclic 1-sila-2,5-diaryltetrazenes which they obtained by the reaction of aryltetrazenes with an excess of a halosilane,[33] and several silatetrazolines have been reported to date.[34] The first stable silaimine $tBu_2Si{=}NSi(tBu)_2$ was presented by Wiberg and co-workers in 1985.[35] *N*-heterocyclic silylene substituted silatetrazolines and silaimines have been observed as products of the reaction of *N*-heterocyclic silylenes with aryl azides.[4b,36] In the case of the Dipp substituted silylene **1**, only a few studies on the reactivity towards azides have been reported so far,[36b,f] and thus we were interested to gain further insight into this field and to compare the results with the well-examined NHSi tBu_2NHSi.

The reaction of $Dipp_2NHSi$ (**1**) with two equivalents of adamantyl azide in hexane led to the formation of a colorless solid which is insoluble in hexane and was identified as 1-$Dipp_2NHSi$-2,5-bis(adamantyl)-tetrazoline (**12**) by NMR spectroscopy, single crystal X-ray diffraction, and elemental analysis (Scheme 5, left). In the ^{29}Si NMR spectrum of **12**, the silicon atom gives rise to a resonance at −52.2 ppm (**12**) which is significantly shifted towards higher fields compared to $Dipp_2NHSi$ (75.9 ppm). The methine protons give rise to one septet at 3.74 ppm, displaying the *pseudo*-C_{2v} symmetry of the

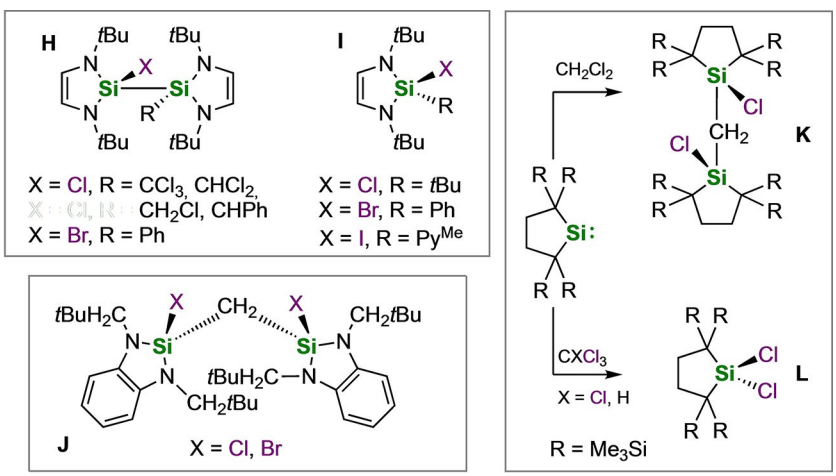

Figure 9. Examples for insertion reactions of *N*-heterocyclic silylenes into carbon–halogen bonds.

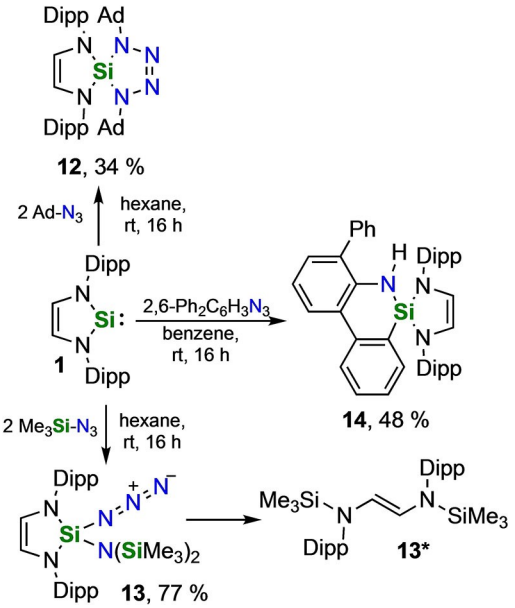

Scheme 5. Reaction of $Dipp_2NHSi$ with the azides Ad-N_3, $(Me)_3Si$-N_3 and 2,6-$(Ph)_2Ph$-N_3 giving the silatetrazoline 1-$Dipp_2NHSi$-2,5-bis(adamantyl)-tetrazoline (**12**), the azido silane (**13**), the degradation product **13*** and the cyclosilamine **14**.

silatetrazoline. Single crystals suitable for X-ray diffraction were grown by slow evaporation of a concentrated benzene solution of **12** at room temperature and the solid-state structure is shown in Figure 10.

Compound **12** consists of a spirocyclic ring system with the former NHSi silicon atom being the spiro atom. The backbone-saturated *tert*-butyl silylenes tBu_2NHSi^{tBu} (1,3,4-tri-*tert*-butyl-1,3-diaza-2-silacyclopent-4-en-2-ylidene) and tBu_2NHSi^{Me} (1,3-di-*tert*-butyl-4,5-dimethyl-1,3-diaza-2-silacyclopent-4-en-2-ylidene) which carry an additional *tert*-butyl or two methyl groups at one carbon atom of the backbone react with adamantyl azide to give also the corresponding tetrazolines.[37] The three tetrazolines show an almost perfect perpendicular arrangement of the two rings (**12**: 88.61(5)°; tBu_2NHSi^{tBu}: 87.39(7)°; tBu_2NHSi^{Me}: 90.00(5)°) with nitrogen-nitrogen bond distances of 1.3823(14) Å (N3–N4), 1.2648(15) Å (N4–N5) and 1.3926(14) Å (N5–N6) and silicon-nitrogen bond lengths of in the range between 1.7167(11) Å and 1.7559(10) Å observed for **12**, which is in line with the aforementioned compounds. For NHCs, various examples are known for the reaction of *in situ* generated NHCs R_2Im (R = Me, iPr, Mes) with alkyl and aryl azides, giving exclusively the respective mono-NHC triazines[38] and bis-NHC triazenyl imidazolium salts,[39] and no NHC-tetrazolines have been observed. Lee and co-workers reported bis-NHC-supported triazenyl radicals which were obtained by reacting 2-chloroimidazolium chlorides with trimethylsilyl azide and subsequent reduction with elemental potassium.[40] Quast *et al.* reported a 1,3-dipolar cycloaddition of a tetrazoline supported carbene with phenyl azide to give a spiro compound consisting of two five-membered rings (**M**, 1,4,9,9-tetramethyl-6-phenyl-1,2,3,4,6,7,8-heptaaza-spiro[4.4]nona-2,7-diene), which is similar to **1** and closely resembles a cyclic NHC-tetrazoline.[41] Comparison of the solid state structures of **M** and **12** reveals similar bond lengths for the nitrogen atoms of the tetrazole backbone (**12**: N3–N4 1.3823(14), N4–N5 1.2648(15), N5–N6 1.3926(14) Å; **M**: N1–N2 1.385(3), N2–N3 1.260(4), N3–N4 1.374(3) Å) and almost identical spiro angles of the two rings (**12**: 88.61(5)°; **M**: 89.28(12)°). The carbon atom of the tetrazole ring of **M**, however, is bent out of the plane of the four nitrogen atoms by 12.82(14)°, whereas in **12**, the silicon atom and the nitrogen atoms are planar (0.24(9)°).

The reaction of **1** with one equivalent of trimethylsilyl azide in hexane resulted in a low yield conversion of **1**. However, the bis(trimethylsilyl)amido azido silane $Dipp_2NHSi(N(SiMe_3)_2)(N_3)$ (**13**) was

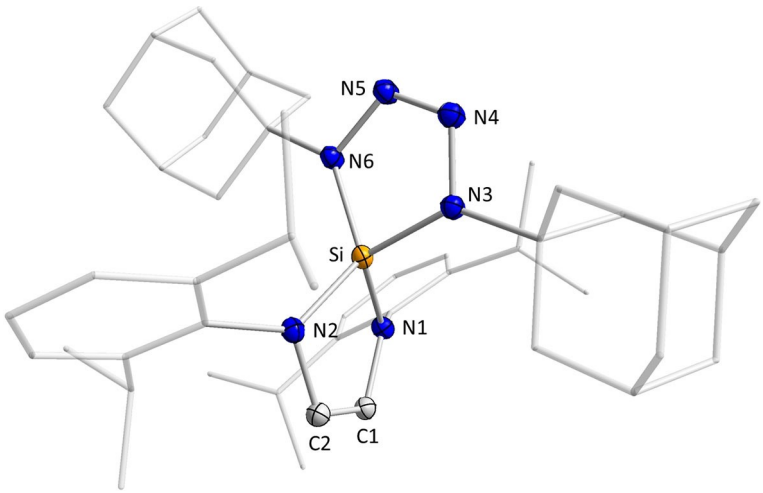

Figure 10. Molecular structure of 1-$Dipp_2NHSi$-2,5-bis(adamantyl)-tetrazoline (**12**) in the solid state (ellipsoids drawn at the 50% probability level; hydrogen atoms omitted for clarity). Selected bond lengths [Å] and angles [°] of **12**: Si–N1 1.7485(10), Si–N2 1.7433(10), N1–C1 1.4238(15), N2–C2 1.4269(15), C1–C2 1.3399(17), Si–N3 1.7559(10), Si–N6 1.7167(11), N3–N4 1.3823(14), N4–N5 1.2648(15), N5–N6 1.3926(14), N1–Si–N2 93.19(5), N1–Si–N3 118.58(5), N6–Si–N2 122.81(5), (N1–C1–C2–N2) / (N1–Si–N2) 21.50(6), (N1–Si–N2) / (N3–Si–N6) 88.61(5), (N3–N4–N5–N6) / (N3–Si–N6) 0.24(9).

isolated in good yields (77%) upon using two equivalents of the azide, as indicated by ^{1}H, ^{29}Si and ^{13}C NMR spectroscopy and elemental analysis. For the *tert*-butyl NHSi *t*Bu$_2$NHSi, the analogous reaction was reported by Denk and co-workers who observed the formation of a silaimine when using one equivalent of trimethylsilyl aizde. The addition of a second equivalent then yielded the silyl azide *t*Bu$_2$NHSi(N(SiMe$_3$)$_2$)(N$_3$).[42] In the ^{29}Si NMR spectrum of **13** two resonances were observed which were assigned to the trimethylsilyl substituents (4.09 ppm) and to the former NHSi silicon atom (**13**: −54.5 ppm; **12**: −52.2 ppm). In the ^{15}N-^{1}H HMBC NMR spectrum of **13**, the nitrogen atoms of the five-membered heterocycle are observed at −299.4 ppm and the trimethylsilyl substituted nitrogen atoms of the amine substituent give rise to one signal at −327.5 ppm. The nitrogen atoms of the azide function were not observed. Single crystals of **13** were obtained by storing a saturated hexane solution of **13** at −30 °C (Figure 11). Furthermore, several attempts to crystallize **13** led to the crystallization of a colorless degradation product, diazabutene **13***, which was formed by cleavage of the silicon–nitrogen bonds of the former NHSi ring (Figure 11).

The silicon atom of the silyl azide Dipp$_2$NHSi(N(SiMe$_3$)$_2$)(N$_3$) (**13**) adopts a distorted tetrahedral structure with an almost planar five-membered ring featuring a C=C double bond (1.327(2) Å). The distances between the nitrogen atoms of the azido substituent are N4–N5 1.222(2) Å and N5–N6 1.136(2) Å and lie in the typical region observed for azide groups.[43] The crystal structure of **13*** clearly reveals a diazabutene, in which the nitrogen atoms are substituted by a trimethylsilyl and a Dipp group. The diazabutene backbone is, as observed for **8**, planar with the SiMe$_3$ silicon atoms barely bend out of the plane (0.1240(4) Å). The C–C′ distance of 1.333(3) Å is in agreement with a C=C double bond (1.34 Å).[21] The angles at the planar, sp^2-hybridized nitrogen atom of Si–N–C 120.84(9)°, Si–N–C1 121.99(9)° and C1–N–C 116.58(11)° add up to 359.41°.

While the reaction of Dipp$_2$NHSi **1** with adamantyl azide led exclusively to the corresponding silatetrazolines **12** and with trimethysilyl azide to compound **13** and the diazabutene **13***, the reaction of **1** with the sterically demanding 2,6-(diphenyl)phenyl azide afforded the C–H activation product **14**. In the ^{1}H NMR spectrum, the resonances of the silylene ring *N*-aryl groups were split, for example two septets were observed at 3.56 and 3.74 ppm for the *iso*propyl methine protons. The silicon atom resonance was detected at −40.1 ppm in the ^{29}Si NMR spectrum. Compound **14** was isolated from hexane as a pale-yellow crystalline solid in 48% yield and the sole formation of **14** was confirmed by elemental analysis. We assume that initially a silaimine is formed which then undergoes a C–H activation to produce the amine function as well as a silicon–carbon bond between the silicon atom and the *ortho* carbon atom of one phenyl substituent of the former azide. X-ray diffraction was performed on single crystals of **14** grown by slow evaporation of a concentrated benzene solution of **14** at room temperature. The solid-state structure of **14** is shown in Figure 12. As observed for **12**, compound **14** is spirocyclic. The two rings of the spiro system are the five-membered NHSi ring and a newly formed six-membered ring made up of the silicon atom, a nitrogen atom of the azide, and four carbon atoms of the (diphenyl)phenyl substituent of the azide. The rings are nearly perpendicular with respect to each other (85.58(8)°).

Conclusion

The reactivity of the *N*-heterocyclic silylene Dipp$_2$NHSi (**1**) with a variety of main group element compounds is presented. The

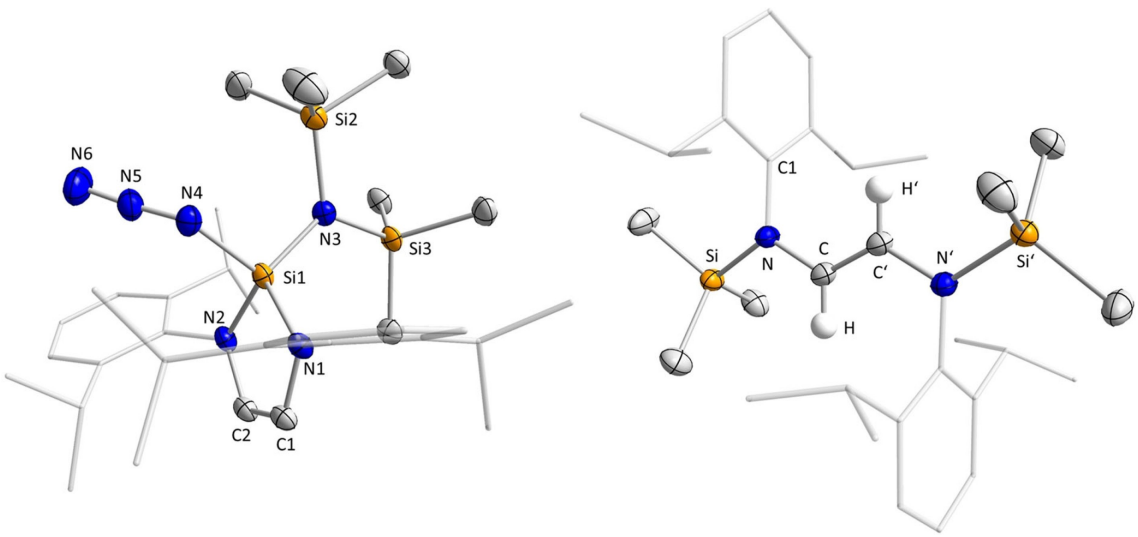

Figure 11. Molecular structure of the **13** (left) and **13*** (right) in the solid state (ellipsoids drawn at the 50% probability level; hydrogen atoms except the hydrogen atoms of the backbone are omitted for clarity). Selected bond lengths [Å] and angles [°] of **13**: Si1–N3 1.7246(14), Si1–N4 1.7480(15), N4–N5 1.222(2), N5–N6 1.136(2), N3–Si2 1.7693(14), N3–Si3 1.7765(14), C1–C2 1.327(2), Si1–N3–N4 104.22(7), Si2–N3–Si3 118.99(8), N1–Si1–N2 93.45(7). Selected bond lengths [Å] and angles [°] of **13***: Si–N 1.7479(12), N–C 1.4151(18), C–C′ 1.333(3), Si-N–C 120.84(9), N–C–C′ 125.81(16), Si-N–C1 121.99(9), C1–N–C 116.58(11), distance Si from (N–C–C′–N′) 0.1240(4).

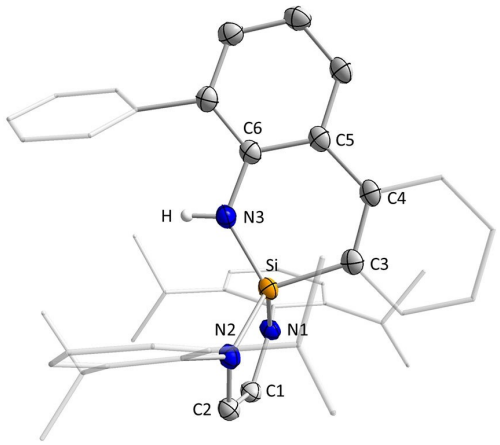

Figure 12. Molecular structure of **14** in the solid state (ellipsoids drawn at the 50% probability level; hydrogen atoms except the amine proton are omitted for clarity). Selected bond lengths [Å] and angles [°] of **14**: Si–N1 1.7372(16), Si–N2 1.7454(15), N1–C1 1.421(2), N2–C2 1.416(2), C1–C2 1.342(3), Si–C3 1.8366(19), Si–N3 1.7101(17), N3–H 0.85(3), C3–C4 1.412(3), C4–C5 1.487(3), C5–C6 1.428(2), C6–N3 1.408(2), N1–Si–N2 91.56(7), C3–Si–N1 112.30(8), N3–Si–N2 114.78(7), (N1–C1–C2–N2) / (N1–Si–N2) 6.86(10), (N1–Si–N2) / (C3–Si–N3) 85.58(8), (C3–C4–C5–C6–N3) / (C3–Si–N3) 5.79(8).

reaction of **1** with AlI_3, $Al(C_6F_5)_3$ and $B(C_6F_5)_3$ afforded the *Lewis* acid/base adducts $Dipp_2NHSi{\cdot}AlI_3$ (**2**) $Dipp_2NHSi{\cdot}Al(C_6F_5)_3$ (**3**) and $Dipp_2NHSi{\cdot}B(C_6F_5)_3$ (**4**). In contrast to the literature-known adduct $tBu_2NHSi{\cdot}B(C_6F_5)_3$, which slowly decomposes with B-C activation to yield a silyl borane, no decomposition of **4** was observed. In contrast to some NHC adducts of alanes and boranes, which readily activate small organic molecules, the NHSi adducts **3** and **4** do not show any detectable FLP reactivity. The reaction with Br_2 and I_2 afforded the dihalo silanes $Dipp_2NHSiBr_2$ (**5**) and $Dipp_2NHSiI_2$ (**6**). The reaction of **1** with Me_3SnCl in a ratio 1:3 led to decomposition of **1** and presumably to the oxidation of the silicon atom with formation of a stannyl silane and the diazabutene $\{(Me_3Sn)N(Dipp)CH\}_2$ (**8**), while reaction with Ph_2SnCl_2 afforded exclusively the chloro silane $Dipp_2NHSiCl_2$ (**7**) and poly(diphenylstannylene) $(Ph_2Sn)_n$. Insertion of **1** into the C–X bond of organohalides was observed for the reaction of **1** with methyl iodide, benzyl chloride, and benzyl bromide leading to $Dipp_2NHSi(I)(CH_3)$ (**9**), $Dipp_2NHSi(Cl)(CH_2Ph)$ (**10**) and $Dipp_2NHSi(Br)(CH_2Ph)$ (**11**). Finally, it was demonstrated that the product of the reaction of **1** with organic azides depends critically on the steric demand of the substituent of the azide. The reaction of **1** with two equivalents of adamantyl azide afforded tetrazoline **12**, which is in accordance with the results obtained previously for tBu_2NHSi and tBu_2NHSi^{H2}. Using the sterically less demanding trimethylsilyl azide, a bis(trimethylsilyl)amino azido silane (**13**), and a degradation product, the diazabutene **13*** was obtained. The reaction of 2,6-(diphenyl) phenyl azide with $Dipp_2NHSi$ gave the cyclosilamine **14**.

Experimental Section

General Procedures. All reactions and subsequent manipulations were performed under an argon atmosphere in an Innovative Technology Inc. glovebox or using standard Schlenk techniques. NMR spectra were recorded on Bruker Avance 300, Bruker Avance 400, Bruker NEO 400 or Bruker Avance 500 spectrometers in C_6D_6 solutions at room temperature if not stated differently. Chemical shifts are listed in parts per million (ppm) and were calibrated against the residual solvent signals (δ (^{1}H): C_6D_5H 7.16; δ (^{13}C): C_6D_6 128.06). Coupling constants are quoted in Hz. Elemental analyses were performed in the micro analytical laboratory of the Institute of Inorganic Chemistry at the University of Würzburg with an Elementar vario MICRO cube. $Dipp_2NHSi$ (**1**)[18,44] was prepared according to literature procedures. All other starting materials were purchased from commercial sources and used without purification. All solvents were HPLC grade, further treated to remove traces of water using an Innovative Technology Inc. Pure-Solv Solvent Purification System and deoxygenated using the freeze-pump-thaw method.

$Dipp_2NHSi{\cdot}AlI_3$ (2). 1,3-Bis(2,6-di*iso*propylphenyl)-1,3-diaza-2-silacyclopent-4-en-2-ylidene (50.0 mg, 124 μmol) and AlI_3 (51.0 mg, 124 μmol) were dissolved in benzene (3 mL) and stirred at room temperature for 16 h. All volatiles were removed *in vacuo*, the remaining solid was washed with hexane (3×2 mL) and evacuated to dryness to yield **2** as an off-white solid (84.5 mg, 108 μmol, 87%).

^{1}H NMR (400.3 MHz, C_6D_6, 300 K): δ [ppm] = 1.08 (d, 12H, $^3J_{H\text{-}H}$ = 6.8 Hz, *i*Pr-CH_3), 1.41 (d, 12H, $^3J_{H\text{-}H}$ = 6.8 Hz, *i*Pr-CH_3), 3.08 (sept, 4H, $^3J_{H\text{-}H}$ = 6.8 Hz, *i*Pr-C*H*), 6.16 (s, 2H, C*H*), 7.08–7.10 (d, 4H, aryl-C*H*), 7.18–7.20 (d, 2H, aryl-C*H*). **^{13}C{^{1}H} NMR** (100.7 MHz, C_6D_6, 300 K): δ [ppm] = 24.5 (*i*Pr-CH_3), 25.2 (*i*Pr-CH_3), 29.4 (*i*Pr-C*H*), 124.4 (aryl-C_{meta}), 126.3 (NCCN), 129.6 (aryl-C_{para}), 136.0 (aryl-C_{ipso}), 145.0 (aryl-C_{ortho}). **^{27}Al NMR** (104.4 MHz, C_6D_6, 300 K): δ [ppm] = 40.1. **^{29}Si{^{1}H} NMR** (79.5 MHz, C_6D_6, 300 K): δ [ppm] = 42.8. **Elemental analysis** No satisfactory elemental analysis was obtained for this compound.

$Dipp_2NHSi{\cdot}Al(C_6F_5)_3$ (3). 1,3-Bis(2,6-di*iso*propylphenyl)-1,3-diaza-2-silacyclopent-4-en-2-ylidene (50.0 mg, 124 μmol) and $Al(C_6F_5)_3$ (65.3 mg, 124 μmol) were dissolved in hexane (4 mL) and toluene (2 mL) and stirred at room temperature for 16 h. All volatiles were removed *in vacuo*, the remaining solid was washed with hexane (3x 2 mL) and evacuated to dryness to yield **3** as a yellow solid (72.3 mg, 77.5 μmol, 63%). **^{1}H NMR** (400.3 MHz, C_6D_6, 300 K): δ [ppm] = 1.03 (d, 12H, $^3J_{H\text{-}H}$ = 6.9 Hz, *i*Pr-CH_3), 1.12 (d, 12H, $^3J_{H\text{-}H}$ = 6.9 Hz, *i*Pr-CH_3), 3.02 (sept, 4H, $^3J_{H\text{-}H}$ = 6.9 Hz, *i*Pr-C*H*), 6.26 (s, 2H, C*H*), 6.99 (d, 4H, $^3J_{H\text{-}H}$ = 7.7 Hz, aryl-C*H*), 7.15 (t, 2H, $^3J_{H\text{-}H}$ = 7.7 Hz, aryl-C*H*). **^{13}C{^{1}H} NMR** (125.8 MHz, C_6D_6, 300 K): δ [ppm] = 22.7 (*i*Pr-CH_3), 25.8 (*i*Pr-CH_3), 29.3 (*i*Pr-C*H*), 124.0 (aryl-*C*), 126.1 (NCCN), 127.2 (aryl-*C*), 129.4 (aryl-*C*), 135.4 (aryl-*C*), 144.9 (aryl-*C*). The resonances of the pentafluorophenyl carbon atoms were not detected. **^{19}F NMR** (376.7 MHz, C_6D_6, 300 K): δ [ppm] = −123.0 (dm, 6F, aryl-C*F*), −150.7 (tt, 3F, aryl-CF_{para}), −160.5 (m, 6F, aryl-C*F*). **^{29}Si{^{1}H} NMR** (79.5 MHz, C_6D_6, 300 K): δ [ppm] = 74.0. **Elemental analysis** (%) calcd. for $C_{44}H_{36}N_2Si\,AlF_{15}$: C 56.65, H 3.89, N 3.00; found C 56.65, H 4.60, N 3.13.

$Dipp_2NHSi{\cdot}B(C_6F_5)_3$ (4). 1,3-Bis(2,6-di*iso*propylphenyl)-1,3-diaza-2-silacyclopent-4-en-2-ylidene (50.0 mg, 124 μmol) and $B(C_6F_5)_3$ (63.3 mg, 124 μmol) were dissolved in hexane (4 mL) and toluene (2 mL) and stirred at room temperature for 16 h. All volatiles were removed *in vacuo*, the remaining solid was washed with hexane (3×2 mL) and evacuated to dryness to yield **4** as a pale-yellow solid (80.4 mg, 87.7 μmol, 71%). Crystals suitable for X-ray diffraction were grown from an at room temperature saturated hexane solution of **4** at −30 °C. **^{1}H NMR** (500.1 MHz, C_6D_6, 30 K): δ [ppm] = 0.96 (d, 12H, $^3J_{H\text{-}H}$ = 6.8 Hz, *i*Pr-CH_3), 1.07 (d, 12H, $^3J_{H\text{-}H}$ = 6.8 Hz, *i*Pr-CH_3), 3.00 (sept, 4H, $^3J_{H\text{-}H}$ = 6.8 Hz, *i*Pr-C*H*), 6.02 (s, 2H, C*H*), 6.90 (d, 4H, $^3J_{H\text{-}H}$ = 7.8 Hz, aryl-CH_{meta}), 7.08 (t, 2H, $^3J_{H\text{-}H}$ = 7.8 Hz, aryl-CH_{para}). **^{11}B{^{1}H} NMR** (160.5 MHz, C_6D_6, 300 K): δ [ppm] = −19.9. **^{13}C NMR** (125.8 MHz, C_6D_6, 300 K): δ [ppm] = 21.9 (qm, $^1J_{C\text{-}H}$ = 126 Hz, *i*Pr-CH_3), 26.1 (qm, $^1J_{C\text{-}H}$ = 126 Hz, *i*Pr-CH_3), 29.5 (dm, $^1J_{C\text{-}H}$ = 126 Hz, *i*Pr-C*H*),

123.4 (m, NCCN), 124.2 (d, $^{1}J_{C\text{-}H}$ = 10.7 Hz, aryl-*C*), 124.7 (m, aryl-*C*), 125.7 (d, $^{1}J_{C\text{-}H}$ = 10.7 Hz, aryl-*C*), 127.7 (s, aryl-*C*), 128.4 (s, aryl-*C*), 129.0 (s, aryl-*C*), 129.6 (s, aryl-*C*), 136.4 (m, aryl-*C*), 136.9 (m, aryl-*C*), 138.4 (m, aryl-*C*), 144.5 (s, aryl-*C*), 147.3 (m, aryl-*C*), 149.2 (m, aryl-*C*). **^{19}F NMR** (160.5 MHz, C_6D_6, 300 K): δ [ppm] = −129.0 (s, 6F, aryl-C*F*), −155.9 (s, 3F, aryl-CF_{para}), −162.2 (s, 6F, aryl-C*F*). **^{29}Si{^{1}H} NMR** (99.4 MHz, C_6D_6, 300 K): δ [ppm] = 72.2. **Elemental analysis** (%) calcd. for $C_{44}H_{36}N_2SiBF_{15}$: C 57.65, H 3.96, N 3.06; found C 57.87, H 4.27, N 2.87.

General procedure for reactions of Dipp$_2$NHSi·Al(C$_6$F$_5$)$_3$ (3) and Dipp$_2$NHSi·B(C$_6$F$_5$)$_3$ (4) in a Young-tap NMR tube. Dipp$_2$NHSi·E(C$_6$F$_5$)$_3$ (E = B, Al; 24.7 μmol) was dissolved in C_6D_6 (0.6 mL) and the respective substrate (24.7 μmol, 1 equivalent) was added. In case of gases, the reactions were carried out at 1 atm after the atmosphere in the NMR tube was exchanged from argon to the gas used using the freeze-pump-thaw method. The reaction mixture was analyzed after 16 h at room temperature using NMR spectroscopy.

1,3-Bis(2,6-di*iso*propylphenyl)-1,3-diaza-2,2-dibromo-2-silacyclopent-4-ene (5). 1,3-Bis(2,6-di*iso*propylphenyl)-1,3-diaza-2-silacyclopent-4-en-2-ylidene (100 mg, 247 μmol) was dissolved in toluene (5 mL), Br_2 (21.7 mg, 7.00 μL, 272 μmol, 1.1 equivalents) was added to the reaction mixture and stirred 16 h at room temperature. All volatiles were removed *in vacuo*, the remaining solid was suspended in hexane (3 mL) and stored at −30 °C to yield **5** as a pale-yellow solid (86.4 mg, 153 μmol, 62 %). Crystals suitable for X-ray diffraction were grown from an at room temperature saturated hexane solution of **5** at −30 °C. **^{1}H NMR** (300.1 MHz, C_6D_6, 298 K): δ [ppm] = 1.18 (d, 12H, $^{3}J_{H\text{-}H}$ = 6.8 Hz, *i*Pr-CH_3), 1.37 (d, 12H, $^{3}J_{H\text{-}H}$ = 6.8 Hz, *i*Pr-CH_3), 3.71 (sept, 4H, $^{3}J_{H\text{-}H}$ = 6.8 Hz, *i*Pr-C*H*), 5.74 (s, 2H, C*H*), 7.11–7.22 (m, 6H, aryl-C*H*). **^{13}C{^{1}H} NMR** (100.7 MHz, C_6D_6, 298 K): δ [ppm] = 24.1 (*i*Pr-CH_3), 26.2 (*i*Pr-CH_3), 28.8 (*i*Pr-*C*H), 120.7 (aryl-C$_{meta}$), 124.6 (NCCN), 128.6 (aryl-C$_{para}$), 135.4 (aryl-C$_{ipso}$), 148.5 (aryl-C$_{ortho}$). **^{29}Si{^{1}H} NMR** (79.5 MHz, C_6D_6, 298 K): δ [ppm] = −59.3. **Elemental analysis** (%) calcd. for $C_{26}H_{36}N_2SiBr_2$: C 55.32, H 6.43, N 4.96; found C 55.58, H 6.66, N 4.54.

1,3-Bis(2,6-di*iso*propylphenyl)-1,3-diaza-2,2-diiodo-2-silacyclopent-4-ene (6). 1,3-Bis(2,6-di*iso*propylphenyl)-1,3-diaza-2-silacyclopent-4-en-2-ylidene (100 mg, 247 μmol) was dissolved in toluene (5 mL), I_2 (34.5 mg, 272 μmol, 1.1 equivalents) was added to the reaction mixture and stirred at room temperature for 16 h. All volatiles were removed *in vacuo*, the remaining solid was suspended in hexane (3 mL) and stored at −30 °C to yield **6** as a pale-yellow solid (92.9 mg, 141 μmol, 57 %). Crystals suitable for X-ray diffraction were grown by slow evaporation of a saturated hexane solution of **6** at room temperature. **^{1}H NMR** (300.1 MHz, C_6D_6, 298 K): δ [ppm] = 1.17 (d, 12H, $^{3}J_{H\text{-}H}$ = 6.8 Hz, *i*Pr-CH_3), 1.42 (d, 12H, $^{3}J_{H\text{-}H}$ = 6.8 Hz, *i*Pr-CH_3), 3.76 (sept, 4H, $^{3}J_{H\text{-}H}$ = 6.8 Hz, *i*Pr-C*H*), 5.77 (s, 2H, C*H*), 7.13–7.27 (m, 6H, aryl-C*H*). **^{13}C{^{1}H} NMR** (101 MHz, C_6D_6, 298 K): δ [ppm] = 24.3 (*i*Pr-CH_3), 26.5 (*i*Pr-CH_3), 29.2 (*i*Pr-*C*H), 121.6 (aryl-C$_{meta}$), 124.8 (NCCN), 128.6 (aryl-C$_{para}$), 135.7 (aryl-C$_{ipso}$), 148.6 (aryl-C$_{ortho}$). **^{29}Si{^{1}H} NMR** (79.5 MHz, C_6D_6, 298 K): δ [ppm] = −134.5. **Elemental analysis** (%) calcd. for $C_{26}H_{36}N_2SiI_2$: C 47.43, H 5.51, N 4.25; found C 45.12, H 5.61, N 4.14. Despite repeated attempts, a satisfactory elemental analysis of compound **6** was not obtained due the high sensitivity of **6** towards air and moisture.

Reaction of Dipp$_2$NHSi (1) with Ph$_2$SnCl$_2$. 1,3-Bis(2,6-di*iso*propylphenyl)-1,3-diaza-2-silacyclopent-4-en-2-ylidene (25.0 mg, 61.8 μmol) and diphenyltin dichloride (21.2 mg, 61.8 μmol, 1 equivalent) were dissolved in C_6D_6 (0.6 mL) in a Young-tap NMR tube. After 16 h at room temperature, the reaction mixture was measured using NMR spectroscopy. Spectra are shown in the Supporting Information. **^{1}H NMR** (500.1 MHz, C_6D_6, 298 K): δ [ppm] = 1.19 (d, 12H, $^{3}J_{H\text{-}H}$ = 6.9 Hz, *i*Pr-CH_3), 1.35 (d, 12H, $^{3}J_{H\text{-}H}$ = 6.9 Hz, *i*Pr-CH_3), 3.67 (sept, 2H, $^{3}J_{H\text{-}H}$ = 6.9 Hz, *i*Pr-C*H*), 5.72 (s, 2H, C*H*), 6.99–7.01 (m, 6H, aryl-C*H*), 7.11–7.12 (m, 7H, aryl-C*H*), 7.17–7.20 (m, 2H, aryl-C*H*), 7.37–7.39 (m, 1H, aryl-C*H*), 7.55–7.57 (m, 1H, aryl-C*H*), 7.62–7.67 (m, 2H, aryl-C*H*). **^{13}C{^{1}H} NMR** (125.8 MHz, C_6D_6, 298 K): δ [ppm] = 24.0 (*i*Pr-CH_3, Dipp$_2$NHSi), 26.1 (*i*Pr-CH_3, Dipp$_2$NHSi), 28.7 (*i*Pr-*C*H, Dipp$_2$NHSi), 119.9 (aryl-C$_{meta}$, Dipp$_2$NHSi), 124.6 (NCCN, Dipp$_2$NHSi), 126.1 (aryl-*C*), 128.4 (aryl-*C*), 128.5 (aryl-*C*), 129.4 (aryl-C$_{para}$, Dipp$_2$NHSi), 129.8 (aryl-*C*), 130.6 (aryl-*C*), 131.7 (aryl-*C*), 135.3 (aryl-C$_{ipso}$, Dipp$_2$NHSi), 136.5 (aryl-*C*), 148.5 (aryl-C$_{ortho}$, Dipp$_2$NHSi). **^{29}Si{^{1}H} NMR** (99.4 MHz, C_6D_6, 298 K): δ [ppm] = −38.2. **^{119}Sn{^{1}H} NMR** (186.5 MHz, C_6D_6, 298 K): δ [ppm] = −218.6, −207.2 ((Ph$_2$Sn)$_6$), −201.5, −201.3, −200.7, −200.2, −200.0, −199.9, −199.8, −199.5, −199.2, −198.6.

1,4-Bis(2,6-di*iso*propylphenyl)-1,4-bis(trimethylstannyl)-1,4-diaza-but-2-ene (8). 1,3-Bis(2,6-di*iso*propylphenyl)-1,3-diaza-2-silacyclopent-4-en-2-ylidene (50.0 mg, 124 μmol) and trimethyltin chloride (74.1 mg, 372 μmol, 3 equivalents) were dissolved in hexane (5 mL) and stirred 1 h at room temperature. All volatiles were removed *in vacuo*, the remaining solid was suspended in hexane (3 mL) and stored at −30 °C to yield **8** as a colorless solid (65 mg, 92.3 μmol, 74 %). Crystals suitable for X-ray diffraction were grown by slow evaporation of a saturated benzene solution of **8** at room temperature. **^{1}H NMR** (400.3 MHz, C_6D_6, 298 K): δ [ppm] = 0.05 (s, 18H, SnCH_3), 1.20 (d, 12H, $^{3}J_{H\text{-}H}$ = 6.9 Hz, *i*Pr-CH_3), 1.44 (d, 12H, $^{3}J_{H\text{-}H}$ = 6.9 Hz, *i*Pr-CH_3), 3.57 (sept, 2H, $^{3}J_{H\text{-}H}$ = 6.9 Hz, *i*Pr-C*H*), 5.28 (s, 2H, C*H*), 7.14–7.19 (m, 6H, aryl-C*H* overlaid by solvent peak). **^{13}C{^{1}H} NMR** (100.7 MHz, C_6D_6, 298 K): δ [ppm] = −6.13 (SnCH_3), 24.8 (*i*Pr-CH_3), 25.3 (*i*Pr-CH_3), 27.8 (*i*Pr-*C*H), 121.6 (aryl-C$_{meta}$), 123.8 (NCCN), 125.8 (aryl-C$_{para}$), 143.8 (aryl-C$_{ipso}$), 148.4 (aryl-C$_{ortho}$). **^{119}Sn{^{1}H} NMR** (186.5 MHz, C_6D_6, 298 K): δ [ppm] = −118.0. **Elemental analysis** (%) calcd. for $C_{32}H_{54}N_2Sn_2$: C 54.58, H 7.73, N 3.98; found C 53.63, H 7.90, N 3.53.

1,3-Bis(2,6-di*iso*propylphenyl)-1,3-diaza-2-iodo-2-methyl-2-silacyclopent-4-en-silane (9). 1,3-Bis(2,6-di*iso*propylphenyl)-1,3-diaza-2-silacyclopent-4-en-2-ylidene (179 mg, 442 μmol) and methyl iodide (144 mg, 50.0 μL, 803 μmol, 1.8 equivalents) were dissolved in hexane (7 mL) and stirred at room temperature for 16 h. All volatiles were removed *in vacuo* and the remaining solid was evacuated to dryness to yield **9** as a colorless solid (195 mg, 357 μmol, 81 %). Crystals suitable for X-ray diffraction were grown from an at room temperature saturated hexane solution of **9** at −30 °C. **^{1}H NMR** (400.3 MHz, C_6D_6, 300 K): δ [ppm] = 0.90 (s, 3H, Si-CH_3), 1.16 (d, 6H, $^{3}J_{H\text{-}H}$ = 6.8 Hz, *i*Pr-CH_3), 1.19 (d, 6H, $^{3}J_{H\text{-}H}$ = 6.8 Hz, *i*Pr-CH_3), 1.19 (d, 6H, $^{3}J_{H\text{-}H}$ = 6.8 Hz, *i*Pr-CH_3), 1.48 (d, 6H, $^{3}J_{H\text{-}H}$ = 6.8 Hz, *i*Pr-CH_3), 3.37 (sept, 2H, $^{3}J_{H\text{-}H}$ = 6.8 Hz, *i*Pr-C*H*), 4.04 (sept, 2H, $^{3}J_{H\text{-}H}$ = 6.8 Hz, *i*Pr-C*H*), 5.75 (s, 2H, C*H*), 7.07 (d, 1H, $^{3}J_{H\text{-}H}$ = 2.3 Hz, aryl-C*H*), 7.09 (d, 1H, $^{3}J_{H\text{-}H}$ = 2.3 Hz, aryl-C*H*), 7.16–7.20 (m, 4H, aryl-C*H*). **^{13}C{^{1}H} NMR** (100.7 MHz, C_6D_6, 300 K): δ [ppm] = 11.5 (Si-CH_3), 23.1 (*i*Pr-CH_3), 25.2 (*i*Pr-CH_3), 26.2 (*i*Pr-CH_3), 26.5 (*i*Pr-CH_3), 28.8 (*i*Pr-*C*H), 28.9 (*i*Pr-CH), 120.5 (NCCN), 124.0 (aryl-*C*H), 125.2 (aryl-*C*H), 128.1 (aryl-*C*H) 136.7 (aryl-*C*H), 148.1 (aryl-*C*), 149.0 (aryl-*C*). **^{29}Si{^{1}H} NMR** (79.5 MHz, C_6D_6, 300 K): δ [ppm] = −30.4. **Elemental analysis** (%) calcd. for $C_{27}H_{39}N_2SiI$: C 59.33, H 7.19, N 5.13; found C 59.28, H 7.21, N 5.01.

1,3-Bis(2,6-di*iso*propylphenyl)-1,3-diaza-2-chloro-2-benzyl-2-silacyclopent-4-en-silane (10). 1,3-Bis(2,6-di*iso*propylphenyl)-1,3-diaza-2-silacyclopent-4-en-2-ylidene (100 mg, 247 μmol) and α-chlorotoluene (31.3 mg, 28.5 μL, 247 μmol) were dissolved in hexane (5 mL) and stirred at room temperature for 16 h. The reaction mixture was concentrated to precipitate a colorless solid. The solvent was decanted, the remaining solid was washed with hexane (2x 1 mL) and dried *in vacuo* to yield **10** as a pale-yellow solid (108 mg, 203 μmol, 82 %). **^{1}H NMR** (400.3 MHz, C_6D_6, 300 K): δ [ppm] = 1.16 (d, 6H, $^{3}J_{H\text{-}H}$ = 6.9 Hz, *i*Pr-CH_3), 1.18 (d, 6H, $^{3}J_{H\text{-}H}$ = 6.8 Hz, *i*Pr-CH_3), 1.26 (d, 6H, $^{3}J_{H\text{-}H}$ = 6.8 Hz, *i*Pr-CH_3), 1.34 (d, 6H, $^{3}J_{H\text{-}H}$ = 6.9 Hz, *i*Pr-CH_3), 2.62 (s, 2H, CH_2), 3.51 (sept, 2H, $^{3}J_{H\text{-}H}$ = 6.9 Hz, *i*Pr-C*H*), 3.92 (sept, 2H, $^{3}J_{H\text{-}H}$ = 6.8 Hz, *i*Pr-C*H*), 5.74 (s, 2H, C*H*), 6.31–6.33 (m, 2H, aryl-C*H*), 6.82–6.83

(m, 2H, aryl-C*H*), 6.94–7.03 (m, 4H, aryl-C*H*), 7.11–7.14 (m, 2H, aryl-C*H*), 7.21–7.25 (m, 2H, aryl-C*H*). **^{13}C{^{1}H} NMR** (100.7 MHz, C_6D_6, 300 K): δ [ppm] = 23.3 (*i*Pr-CH_3), 24.3 (*i*Pr-CH_3), 25.8 (*i*Pr-CH_3), 26.1 (CH_2), 26.6 (*i*Pr-CH_3), 28.4 (*i*Pr-CH), 28.8 (*i*Pr-C*H*), 119.8 (NCCN), 124.1 (aryl-C*H*), 124.9 (aryl-CH), 125.4 (aryl-C*H*), 128.0 (aryl-C*H*), 128.4 (aryl-C*H*), 129.9 (aryl-C*H*), 134.9 (aryl-*C*), 137.6 (aryl-*C*), 148.1 (aryl-*C*), 149.0 (aryl-*C*). **^{29}Si{^{1}H} NMR** (79.5 MHz, C_6D_6, 300 K): δ [ppm] = −19.4. **Elemental analysis** (%) calcd. for $C_{33}H_{43}N_2SiCl$: C 74.61, H 8.16, N 5.27; found C 74.02, H 8.20, N 5.16.

1,3-Bis(2,6-di*iso*propylphenyl)-1,3-diaza-2-bromo-2-benzyl-2-sila-cyclopent-4-en-silane (11). 1,3-Bis(2,6-di*iso*propylphenyl)-1,3-diaza-2-silacyclopent-4-en-2-ylidene (100 mg, 247 μmol) and α-bromotoluene (42.2 mg, 29.3 μL, 247 μmol) were dissolved in hexane (5 mL) and stirred at room temperature for 16 h. The reaction mixture was concentrated to precipitate a colorless solid. The solvent was decanted, the remaining solid was washed with hexane (2x 1 mL) and dried in vacuo to yield **11** as a pale-yellow solid (107 mg, 186 µmol, 75 %). Crystals suitable for X-ray diffraction were grown by vapor diffusion of hexane into a saturated solution of **11** in 1,2-difluoro benzene. **^{1}H NMR** (400.3 MHz, C_6D_6, 300 K): δ [ppm] = 1.16 (d, 6H, $^{3}J_{H\text{-}H}$ = 6.9 Hz, *i*Pr-CH_3), 1.23 (d, 6H, $^{3}J_{H\text{-}H}$ = 6.7 Hz, *i*Pr-CH_3), 1.24 (d, 6H, $^{3}J_{H\text{-}H}$ = 6.7 Hz, *i*Pr-CH_3), 1.33 (d, 6H, $^{3}J_{H\text{-}H}$ = 6.9 Hz, *i*Pr-CH_3), 2.73 (s, 2H, CH_2), 3.52 (sept, 2H, $^{3}J_{H\text{-}H}$ = 6.9 Hz, *i*Pr-C*H*), 3.98 (sept, 2H, $^{3}J_{H\text{-}H}$ = 6.9 Hz, *i*Pr-C*H*), 5.76 (s, 2H, C*H*), 6.31–6.33 (m, 2H, aryl-C*H*), 6.82–6.84 (m, 2H, aryl-C*H*), 7.14–7.16 (m, 3H, aryl-C*H*), 7.17–7.17 (m, 1H, aryl-C*H*), 7.22–7.25 (m, 2H, aryl-C*H*). **^{13}C{^{1}H} NMR** (100.7 MHz, C_6D_6, 300 K): δ [ppm] = 23.2 (*i*Pr-CH_3), 24.5 (*i*Pr-CH_3), 26.0 (*i*Pr-CH_3), 26.7 (*i*Pr-CH_3), 28.3 (CH_2), 28.5 (*i*Pr-CH), 28.8 (*i*Pr-C*H*), 120.1 (NCCN), 124.1 (aryl-C*H*), 125.1 (aryl-CH), 125.6 (aryl-C*H*), 128.4 (aryl-C*H*), 130.2 (aryl-C*H*), 134.8 (aryl-*C*), 137.5 (aryl-*C*), 148.1 (aryl-*C*), 149.1 (aryl-*C*). **^{29}Si{^{1}H} NMR** (79.5 MHz, C_6D_6, 300 K): δ [ppm] = −20.9. **Elemental analysis** (%) calcd. for $C_{33}H_{43}N_2SiBr$: C 68.85, H 7.53, N 4.87; found C 68.85, H 8.00, N 4.63.

1-Dipp$_2$NHSi-2,5-bis(adamantyl)-tetrazoline (12). 1,3-Bis(2,6-di*iso*propylphenyl)-1,3-diaza-2-silacyclopent-4-en-2-ylidene (50.0 mg, 124 μmol) and 1-azidoadamantane (43.8 mg, 247 μmol, 2 equivalents) were dissolved in hexane (7 mL) and stirred at room temperature for 16 h. The precipitate was filtered off, washed with hexane (3x 3 mL) and dried *in vacuo* to yield **12** as a colorless solid (30.8 mg, 42.1 μmol, 34 %). Crystal suitable for X-ray diffraction were grown by slow evaporation of a concentrated benzene solution of **12** at room temperature. **^{1}H NMR** (400.3 MHz, C_6D_6, 300 K): δ [ppm] = 1.27 (d, 24H, $^{3}J_{H\text{-}H}$ = 6.6 Hz, *i*Pr-CH_3), 1.50 (s, 12H, Ad-CH_2), 1.95 (s, 6H, Ad-C*H*), 2.12 (s, 12H, $^{3}J_{H\text{-}H}$ = 6.9 Hz, Ad-CH_2), 3.74 (sept, 4H, $^{3}J_{H\text{-}H}$ = 6.6 Hz, *i*Pr-C*H*), 5.66 (s, 2H, C*H*), 7.10–7.18 (m, 6H, aryl-C*H*, overlaid by solvent peak). **^{13}C{^{1}H} NMR** (100.7 MHz, C_6D_6, 300 K): δ [ppm] = 24.9 (*i*Pr-CH_3), 26.9 (*i*Pr-CH_3), 28.6 (*i*Pr-CH), 36.5 (Ad-CH_2), 42.4 (Ad-CH_2), 55.8 (Ad-CH), 117.9 (aryl-C_{meta}), 125.6 (NCCN), 125.8 (aryl-C_{para}), 139.4 (aryl-C_{ipso}), 145.4 (aryl-C_{ortho}). **^{29}Si{^{1}H} NMR** (99.4 MHz, C_6D_6, 300 K): δ [ppm] = −52.2. **Elemental analysis** (%) calcd. for $C_{46}H_{66}N_6Si$: C 75.57, H 9.10, N 11.49; found C 75.36, H 9.39, N 11.58.

Bis(trimethylsilyl)amido azido silane (13). 1,3-Bis(2,6-di*iso*propylphenyl)-1,3-diaza-2-silacyclopent-4-en-2-ylidene (50.0 mg, 124 μmol) and trimethylsilyl azide (28.6 mg, 32.9 µL, 248 μmol, 2 equivalents) were dissolved in hexane (5 mL) and stirred at room temperature for 16 h. All volatiles were removed *in vacuo* to yield **13** as a yellow solid (58.6 mg, 96.5 μmol, 77 %). Crystals suitable for X-ray diffraction were grown from an at room temperature saturated hexane solution of **13** at −30 °C. **^{1}H NMR** (400.3 MHz, C_6D_6, 300 K): δ [ppm] = 0.26 (s, 18H, Si-CH_3), 1.21 (d, 6H, $^{3}J_{H\text{-}H}$ = 6.7 Hz, *i*Pr-CH_3), 1.28 (d, 6H, $^{3}J_{H\text{-}H}$ = 6.7 Hz, *i*Pr-CH_3), 1.35 (d, 6H, $^{3}J_{H\text{-}H}$ = 6.8 Hz, *i*Pr-CH_3), 1.49 (d, 6H, $^{3}J_{H\text{-}H}$ = 6.7 Hz, *i*Pr-CH_3), 3.71 (sept, 2H, $^{3}J_{H\text{-}H}$ = 6.7 Hz, *i*Pr-C*H*), 3.73 (sept, 2H, $^{3}J_{H\text{-}H}$ = 6.8 Hz, *i*Pr-C*H*), 5.61 (s, 2H, C*H*), 7.11–7.20 (m, 6H, aryl-C*H*). **^{13}C{^{1}H} NMR** (100.7 MHz, C_6D_6, 300 K): δ [ppm] = 5.35 (Si-CH_3), 24.3 (*i*Pr-CH_3), 26.6 (*i*Pr-CH_3), 27.1 (*i*Pr-CH_3), 28.4 (*i*Pr-CH), 29.0 (*i*Pr-CH), 120.2 (aryl-*C*), 124.2 (NCCN), 125.6 (aryl-*C*), 127.2 (aryl-*C*), 138.9 (aryl-*C*), 148.1 (aryl-*C*), 148.6 (aryl-*C*). **^{15}N-^{1}H COSY NMR** (50.7 Hz / 500.1 Hz, C_6D_6, 300 K): δ [ppm] = −327.5 (*N*-$SiMe_3$), −299.4 (*N*-Dipp). **^{29}Si{^{1}H} NMR** (79.5 MHz, C_6D_6, 300 K): δ [ppm] = 4.09 (*Si*-CH_3), −54.4 (N-*Si*-N). **Elemental analysis** (%) calcd. for $C_{32}H_{54}N_6Si_2$: C 63.31, H 8.97, N 13.84; found C 61.73, H 8.88, N 11.60.

Cyclosilamine (14). 1,3-Bis(2,6-di*iso*propylphenyl)-1,3-diaza-2-silacyclopent-4-en-2-ylidene (30.0 mg, 74.1 μmol) and 2,6-(diphenyl) phenylazide (20.1 mg, 74.1 μmol) were dissolved in benzene (5 mL) and stirred at room temperature for 16 h. All volatiles were removed *in vacuo*, the remaining solid was dissolved in hexane (3 mL) and stored at −30 °C to yield **14** as a light yellow crystalline solid (22.8 mg, 35.2 μmol, 48 %). Crystal suitable for X-ray diffraction were grown by slow evaporation of a concentrated benzene solution of **14** at room temperature. **^{1}H NMR** (500.1 MHz, C_6D_6, 300 K): δ [ppm] = 0.67 (d, 6H, $^{3}J_{H\text{-}H}$ = 6.8 Hz, *i*Pr-CH_3), 0.89 (t, 3H, $^{3}J_{H\text{-}H}$ = 7.2 Hz, *i*Pr-CH_3), 0.92 (d, 6H, $^{3}J_{H\text{-}H}$ = 6.8 Hz, *i*Pr-CH_3), 1.25 (t, 12H, $^{3}J_{H\text{-}H}$ = 7.2 Hz, *i*Pr-CH_3), 3.57 (sept, 2H, $^{3}J_{H\text{-}H}$ = 6.8 Hz, *i*Pr-C*H*), 3.75 (sept, 2H, $^{3}J_{H\text{-}H}$ = 6.8 Hz, *i*Pr-C*H*), 5.39 (s, 1H, N*H*), 5.75 (s, 2H, C*H*), 6.72 (dd, 1H, $^{3}J_{H\text{-}H}$ = 8.1 Hz, aryl-C*H*), 6.88 (dd, 1H, $^{3}J_{H\text{-}H}$ = 7.3 Hz, aryl-C*H*), 6.96 (dd, 2H, $^{3}J_{H\text{-}H}$ = 7.3 Hz, aryl-C*H*), 7.00 (m, 1H, aryl-C*H*), 7.02 (m, 1H, aryl-C*H*), 7.05 (m, 3H, aryl-C*H*), 7.08 (m, 1H, aryl-C*H*), 7.09 (m, 1H, aryl-C*H*), 7.11 (m, 1H, aryl-C*H*), 7.12 (m, 1H, aryl-C*H*), 7.14 (m, 1H, aryl-C*H*), 7.76 (dm, 1H, aryl-C*H*), 7.83 (d, 1H, $^{3}J_{H\text{-}H}$ = 8.1 Hz, aryl-C*H*), 8.35 (dd, 1H, $^{3}J_{H\text{-}H}$ = 8.1 Hz, aryl-C*H*). **^{13}C{^{1}H} NMR** (125.8 MHz, C_6D_6, 300 K): δ [ppm] = 14.4, 23.1 (*i*Pr-CH_3), 24.0 (*i*Pr-CH_3), 24.3, 25.4 (*i*Pr-CH_3), 26.2 (*i*Pr-CH_3), 28.5 (*i*Pr-CH), 28.7 (*i*Pr-C*H*), 32.0, 119.2, 119.2 (NCCN), 121.7 (aryl-C*H*), 124.1 (aryl-C*H*), 124.1 (aryl-C*H*), 124.3 (aryl-C*H*), 125.8 (aryl-CH), 125.8 (aryl-C*H*), 126.9 (aryl-C*H*), 126.9 (aryl-C*H*), 127.7 (aryl-C*H*), 128.4 (aryl-C*H*), 128.7 (aryl-C*H*), 129.5 (aryl-C*H*), 130.2 (aryl-C*H*), 131.2 (aryl-C*H*), 131.2 (aryl-C*H*), 132.0 (aryl-*C*), 136.3 (aryl-C*H*), 138.9 (aryl-*C*), 139.9 (aryl-*C*), 140.0 (aryl-*C*), 142.9 (aryl-*C*), 147.6 (aryl-*C*), 148.0 (aryl-*C*). **^{29}Si{^{1}H} NMR** (79.5 MHz, C_6D_6, 300 K): δ [ppm] = −40.1. **Elemental analysis** (%) calcd. for $C_{44}H_{49}N_3Si$: C 81.56, H 7.62, N 6.48; found C 81.28, H 7.91, N 6.50.

Crystallographic Details

Crystal data were collected with two Bruker D8 Apex-2 diffractometers equipped with an Oxford Cryosystems low-temperature device using a CCD area detector and graphite or multilayer monochromated Mo-K_α radiation or a Rigaku XtaLAB Synergy-DW diffractometer equipped with an Oxford Cryo 800 using a HyPix-6000HE detector and copper monochromated Cu-K_α radiation. Crystals were immersed in a film of perfluoropolyether oil on a MicroMount™ and data were collected at 100 K. The images were processed with the Bruker or CrySalis software packages and the structures solved using the ShelXTL software package. All non-hydrogen atoms were refined anisotropically. Hydrogen atoms were included in structure factor calculations and assigned to idealized positions.

Crystal data for 4: $C_{44}H_{36}BF_{15}N_2Si$, M_r = 1426.27, T = 100.00(10) K, λ = 0.77073 Å, yellow block, 0.100×0.146×0.359 mm^3, triclinic space group $P\bar{1}$, a = 13.6485(10), b = 17.6582(12) Å, c = 18.8693(13) Å, α = 106.855(3), β = 107.231(3), γ = 92.482(3), V = 4115.2(5) Å^3, Z = 4, ρ_{calcd} = 1.480 Mg/m^3, μ = 0.161 mm^{-1}, F(000) = 1872, 94302 reflections, $-18 \le h \le 18$, $-23 \le k \le 23$, $-25 \le l \le 25$, $1.191 < \theta < 28.494°$, completeness 99.5 %, 20757 independent reflections, 12424 reflections observed with [$I > 2\sigma(I)$], 1151 parameters, 0 restraints, R indices (all data) R_1 = 0.1127, wR_2 = 0.1256, final R indices [$I > 2\sigma(I)$] R_1 = 0.0530, wR_2 = 0.1074, largest difference peak and hole 0.760 and −0.446 eA^{-3}, GooF = 1.015.

Crystal data for 5: $C_{26}H_{36}N_2Br_2Si$, $M_r = 564.48$, T = 100 K, $\lambda = 0.71073$ Å, yellow plate, $0.120 \times 0.257 \times 0.704$ mm^3, orthorhombic space group Pnma, $a = 12.0901(7)$ Å, $b = 21.0717(13)$ Å, $c = 10.4566(7)$ Å, V = 2663.9(3) Å^3, Z = 4, $\rho_{calcd} = 1.407$ Mg/m^3, $\mu = 3.104$ mm^{-1}, F(000) = 1160, 40509 reflections, $-16 \le h \le 16$, $-28 \le k \le 28$, $-13 \le l \le 13$, $1.933 < \theta < 28.309°$, completeness 99.9%, 3392 independent reflections, 2745 reflections observed with $[I > 2\sigma(I)]$, 149 parameters, 0 restraints, R indices (all data) $R_1 = 0.0454$, $wR_2 = 0.1047$, final R indices $[I > 2\sigma(I)]$ $R_1 = 0.0340$, $wR_2 = 0.0976$, largest difference peak and hole 0.556 and −1.247 eA^{-3}, GooF = 1.030.

Crystal data for 6: $C_{26}H_{36}N_2I_2Si$, $M_r = 638.46$, T = 100.00(11) K, $\lambda = 1.54184$ Å, yellow block, $0.178 \times 0.224 \times 0.280$ mm^3, orthorhombic space group Pnma, $a = 12.36420(10)$ Å, $b = 21.01450(10)$ Å, $c = 10.48310(10)$ Å, V = 2723.80(4) Å^3, Z = 8, $\rho_{calcd} = 1.606$ Mg/m^3, $\mu = 18.662$ mm^{-1}, F(000) = 1304, 54381 reflections, $-14 \le h \le 15$, $-25 \le k \le 25$, $-12 \le l \le 11$, $4.208 < \theta < 72.127°$, completeness 100%, 2753 independent reflections, 2743 reflections observed with $[I > 2\sigma(I)]$, 150 parameters, 0 restraints, R indices (all data) $R_1 = 0.0277$, $wR_2 = 0.0748$, final R indices $[I > 2\sigma(I)]$ $R_1 = 0.0277$, $wR_2 = 0.0748$, largest difference peak and hole 1.142 and −1.094 eA^{-3}, GooF = 1.051.

Crystal data for 8: $C_{32}H_{54}N_2Sn_2$, $M_r = 704.15$, T = 100.01(10) K, $\lambda = 1.54184$ Å, colorless block, $0.059 \times 0.071 \times 0.266$ mm^3, orthorhombic space group $P2_12_12_1$, $a = 8.6820(2)$ Å, $b = 17.5960(3)$ Å, $c = 21.9586(5)$ Å, V = 3354.58(12) Å^3, Z = 4, $\rho_{calcd} = 1.394$ Mg/m^3, $\mu = 11.979$ mm^{-1}, F(000) = 1440, 66727 reflections, $-10 \le h \le 10$, $-19 \le k \le 21$, $-26 \le l \le 27$, $3.218 < \theta < 72.123°$, completeness 1.77/1.00, 6613 independent reflections, 6452 reflections observed with $[I > 2\sigma(I)]$, 339 parameters, 0 restraints, R indices (all data) $R_1 = 0.0418$, $wR_2 = 0.1039$, final R indices $[I > 2\sigma(I)]$ $R_1 = 0.0405$, $wR_2 = 0.1034$, largest difference peak and hole 1.868 and −1.387 eA^{-3}, GooF = 1.036.

Crystal data for 9: $C_{27}H_{39}N_2ISi$, $M_r = 437.27$, T = 100(2) K, $\lambda = 1.54184$ Å, colorless plate, $0.042 \times 0.076 \times 0.385$ mm^3, orthorhombic space group Pnma, $a = 12.23390(10)$, $b = 21.0553(2)$ Å, $c = 10.49910(10)$ Å, V = 2704.45(4) Å^3, Z = 5, $\rho_{calcd} = 1.342$ Mg/m^3, $\mu = 9.831$ mm^{-1}, F(000) = 1128, 53020 reflections, $-15 \le h \le 11$, $-25 \le k \le 25$, $-12 \le l \le 12$, $4.199 < \theta < 72.122°$, completeness 100%, 2729 independent reflections, 2652 reflections observed with $[I > 2\sigma(I)]$, 144 parameters, 0 restraints, R indices (all data) $R_1 = 0.0219$, $wR_2 = 0.0564$, final R indices $[I > 2\sigma(I)]$ $R_1 = 0.0213$, $wR_2 = 0.0561$, largest difference peak and hole 0.917 and −0.378 eA^{-3}, GooF = 1.062.

Crystal data for 11: $C_{33}H_{43}N_2BrSi$, $M_r = 575.69$, T = 100.00(10) K, $\lambda = 1.54184$ Å, colorless plate, $0.042 \times 0.096 \times 0.304$ mm^3, orthorhombic space group $P2_12_12_1$, $a = 9.1730(2)$, $b = 16.9984(3)$ Å, $c = 19.4498(4)$ Å, V = 3032.74(11) Å^3, Z = 4, $\rho_{calcd} = 1.261$ Mg/m^3, $\mu = 2.389$ mm^{-1}, F(000) = 1216, 17331 reflections, $-10 \le h \le 11$, $-20 \le k \le 12$, $-23 \le l \le 24$, $3.453 < \theta < 72.125°$, completeness 1.72/0.97, 5786 independent reflections, 5481 reflections observed with $[I > 2\sigma(I)]$, 342 parameters, 6 restraints, R indices (all data) $R_1 = 0.0525$, $wR_2 = 0.1388$, final R indices $[I > 2\sigma(I)]$ $R_1 = 0.0499$, $wR_2 = 0.1369$, largest difference peak and hole 0.552 and −0.859 eA^{-3}, GooF = 1.052.

Crystal data for 12: $C_{46}H_{66}N_6Si$, $M_r = 916.65$, T = 100.00(10) K, $\lambda = 1.54184$ Å, colorless block, $0.057 \times 0.123 \times 0.226$ mm^3, monoclinic space group $P2_1/c$, $a = 20.27630(10)$, $b = 40.3564(3)$ Å, $c = 10.10800(10)$ Å, $\beta = 102.5260(10)$, V = 8074.29(11) Å^3, Z = 4, $\rho_{calcd} = 1.203$ Mg/m^3, $\mu = 0.811$ mm^{-1}, F(000) = 3184, 96524 reflections, $-25 \le h \le 25$, $-49 \le k \le 49$, $-10 \le l \le 12$, $2.486 < \theta < 72.127°$, completeness 99.9%, 15903 independent reflections, 13964 reflections observed with $[I > 2\sigma(I)]$, 971 parameters, 0 restraints, R indices (all data) $R_1 = 0.0442$, $wR_2 = 0.1089$, final R indices $[I > 2\sigma(I)]$ $R_1 = 0.0383$, $wR_2 = 0.1021$, largest difference peak and hole 0.313 and −0.380 eA^{-3}, GooF = 1.037.

Crystal data for 13: $C_{32}H_{54}N_6Si_3$, $M_r = 607.08$, T = 100.00(10) K, $\lambda = 1.54184$ Å, colorless block, $0.105 \times 0.194 \times 0.290$ mm^3, triclinic space group $P\bar{1}$, $a = 9.1235(2)$, $b = 9.8699(2)$ Å, $c = 20.0995(2)$ Å, $\alpha = 79.6860(10)$, $\beta = 88.1520(10)$, $\gamma = 83.612(2)$, V = 1769.48(6) Å^3, Z = 2, $\rho_{calcd} = 1.139$ Mg/m^3, $\mu = 1.454$ mm^{-1}, F(000) = 660, 66230 reflections, $-11 \le h \le 11$, $-12 \le k \le 12$, $-24 \le l \le 24$, $2.234 < \theta < 72.129°$, completeness 99.7%, 6964 independent reflections, 6445 reflections observed with $[I > 2\sigma(I)]$, 384 parameters, 0 restraints, R indices (all data) $R_1 = 0.0465$, $wR_2 = 0.1314$, final R indices $[I > 2\sigma(I)]$ $R_1 = 0.0442$, $wR_2 = 0.1294$ largest difference peak and hole 0.688 and −0.315 eA^{-3}, GooF = 1.047.

Crystal data for 13*: $C_{32}H_{34}N_2Si_2$, $M_r = 522.94$, T = 100.01(10) K, $\lambda = 1.54184$ Å, colorless block, $0.142 \times 0.180 \times 0.252$ mm^3, triclinic space group $P\bar{1}$, $a = 8.7119(2)$, $b = 9.4161(2)$ Å, $c = 11.2448(2)$ Å, $\alpha = 103.215(2)$, $\beta = 91.540(2)$, $\gamma = 114.401(2)$, V = 810.10(3) Å^3, Z = 2, $\rho_{calcd} = 1.072$ Mg/m^3, $\mu = 1.135$ mm^{-1}, F(000) = 288, 16069 reflections, $-10 \le h \le 10$, $-11 \le k \le 9$, $-13 \le l \le 13$, $4.077 < \theta < 72.110°$, completeness 99.7%, 3172 independent reflections, 2987 reflections observed with $[I > 2\sigma(I)]$, 170 parameters, 0 restraints, R indices (all data) $R_1 = 0.0542$, $wR_2 = 0.1417$, final R indices $[I > 2\sigma(I)]$ $R_1 = 0.0525$, $wR_2 = 0.1400$ largest difference peak and hole 0.895 and −0.340 eA^{-3}, GooF = 1.056.

Crystal data for 14: $C_{50}H_{55}N_3Si$, $M_r = 726.06$, T = 100.00(10) K, $\lambda = 1.54184$ Å, colorless block, $0.058 \times 0.162 \times 0.205$ mm^3, monoclinic space group $P2_1/c$, $a = 16.0677(2)$, $b = 19.3165(3)$ Å, $c = 13.16640(10)$ Å, $\beta = 94.6510(10)$, V = 4073.02(9) Å^3, Z = 4, $\rho_{calcd} = 1.184$ Mg/m^3, $\mu = 0.788$ mm^{-1}, F(000) = 1560, 47944 reflections, $-19 \le h \le 19$, $-23 \le k \le 23$, $-15 \le l \le 16$, $2.759 < \theta < 72.123°$, completeness 100%, 8023 independent reflections, 7078 reflections observed with $[I > 2\sigma(I)]$, 499 parameters, 0 restraints, R indices (all data) $R_1 = 0.0600$, $wR_2 = 0.1463$, final R indices $[I > 2\sigma(I)]$ $R_1 = 0.0529$, $wR_2 = 0.1381$, largest difference peak and hole 0.557 and −0.414 eA^{-3}, GooF = 1.009.

Deposition Numbers 2036027 (**4**), 2036025 (**5**), 2036026 (**6**) 2036025 (**8**), 2036021 (**9**), 2036020 (**11**), 2036024 (**12**), 2036029 (**13**) 2036022 (**13***) and 2036028 (**14**) contain the supplementary crystallographic data for this paper. These data are provided free of charge by the joint Cambridge Crystallographic Data Centre and Fachinformationszentrum Karlsruhe Access Structures service www.ccdc.cam.ac.uk/structures.

Acknowledgement

This work was supported by the Julius-Maximilians-Universität Würzburg. Open access funding enabled and organized by Projekt DEAL.

Conflict of Interest

The authors declare no conflict of interest.

Keywords: Carbenes · E–X bond activation · *Lewis* acid/base adducts · Organoazides · Silylenes

[1] M. Denk, R. Lennon, R. Hayashi, R. West, A. V. Belyakov, H. P. Verne, A. Haaland, M. Wagner, N. Metzler, *J. Am. Chem. Soc.* **1994**, *116*, 2691–2692.

[2] a) S. Raoufmoghaddam, Y.-P. Zhou, Y. Wang, M. Driess, *J. Organomet. Chem.* **2017**, *829*, 2–10; b) B. Blom, M. Stoelzel, M. Driess, *Chem. Eur. J.* **2013**, *19*, 40–62.

[3] a) L. J. Murphy, K. N. Robertson, J. D. Masuda, J. A. C. Clyburne, *N-Heterocyclic Carbenes: Effective Tools for Organometallic Synthesis* (Ed.: S. P. Nolan), Wiley-VCH, **2014**, pp. 427–497; b) V. Nesterov, D. Reiter, P.

Bag, P. Frisch, R. Holzner, A. Porzelt, S. Inoue, *Chem. Rev.* **2018**, *118*, 9678–9842; c) K. Xu, Z. Wang, T. Zhu, *Synlett* **2020**, *31*, 925–932.
[4] a) S. B. Clendenning, B. Gehrhus, P. B. Hitchcock, D. F. Moser, J. F. Nixon, R. West, *J. Chem. Soc. Dalton Trans.* **2002**, 484–490; b) N. J. Hill, D. F. Moser, I. A. Guzei, R. West, *Organometallics* **2005**, *24*, 3346–3349; c) D. F. Moser, A. Naka, I. A. Guzei, T. Müller, R. West, *J. Am. Chem. Soc.* **2005**, *127*, 14730–14738; d) H. Braunschweig, T. Brückner, A. Deissenberger, R. D. Dewhurst, A. Gackstatter, A. Gärtner, A. Hofmann, T. Kupfer, D. Prieschl, T. Thiess, S. R. Wang, *Chem. Eur. J.* **2017**, *23*, 9491–9494; e) H.-C. Tsai, Y.-F. Lin, W.-C. Liu, G.-H. Lee, S.-M. Peng, C.-W. Chiu, *Organometallics* **2017**, *36*, 3879–3882.
[5] a) M. J. Krahfuss, J. Nitsch, F. M. Bickelhaupt, T. B. Marder, U. Radius, *Chem. Eur. J.* **2020**, *26*, 11276–11292; b) M. J. Krahfuss, U. Radius, *Inorg. Chem.* **2020**, *59*, 10976–10985.
[6] a) V. Lavallo, Y. Canac, C. Präsang, B. Donnadieu, G. Bertrand, *Angew. Chem. Int. Ed.* **2005**, *44*, 5705–5709; *Angew. Chem.* **2005**, *117*, 5851–5855; b) U. S. D. Paul, U. Radius, *Eur. J. Inorg. Chem.* **2017**, 3362–3375; c) U. S. D. Paul, M. J. Krahfuss, U. Radius, *Chem. Unserer Zeit* **2019**, *53*, 212–223.
[7] a) S. Kronig, E. Theuergarten, D. Holschumacher, T. Bannenberg, C. G. Daniliuc, P. G. Jones, M. Tamm, *Inorg. Chem.* **2011**, *50*, 7344–7359; b) D. Holschumacher, T. Bannenberg, C. G. Hrib, P. G. Jones, M. Tamm, *Angew. Chem. Int. Ed.* **2008**, *47*, 7428–7432; *Angew. Chem.* **2008**, *120*, 7538–7542; c) A. Winkler, M. Freytag, P. G. Jones, M. Tamm, *J. Organomet. Chem.* **2015**, *775*, 164–168; d) G. C. Welch, R. R. San Juan, J. D. Masuda, D. W. Stephan, *Science* **2006**, *314*, 1124–1126.
[8] B. Birkmann, T. Voss, S. J. Geier, M. Ullrich, G. Kehr, G. Erker, D. W. Stephan, *Organometallics* **2010**, *29*, 5310–5319.
[9] a) J. S. J. McCahill, G. C. Welch, D. W. Stephan, *Angew. Chem. Int. Ed.* **2007**, *46*, 4968–4971; *Angew. Chem.* **2007**, *119*, 5056–5059; b) A. Stirling, A. Hamza, T. A. Rokob, I. Papai, *Chem. Commun.* **2008**, 3148–3150; c) M. A. Dureen, D. W. Stephan, *J. Am. Chem. Soc.* **2009**, *131*, 8396–8397; d) T. Voss, C. Chen, G. Kehr, E. Nauha, G. Erker, D. W. Stephan, *Chem. Eur. J.* **2010**, *16*, 3005–3008.
[10] C. M. Mömming, E. Otten, G. Kehr, R. Fröhlich, S. Grimme, D. W. Stephan, G. Erker, *Angew. Chem. Int. Ed.* **2009**, *48*, 6643–6646; *Angew. Chem.* **2009**, *121*, 6770–6773.
[11] S. Porcel, G. Bouhadir, N. Saffon, L. Maron, D. Bourissou, *Angew. Chem. Int. Ed.* **2010**, *49*, 6186–6189; *Angew. Chem.* **2010**, *122*, 6322–6325.
[12] G. Schnee, O. Nieto Faza, D. Specklin, B. Jacques, L. Karmazin, R. Welter, C. Silva Lopez, S. Dagorne, *Chem. Eur. J.* **2015**, *21*, 17959–17972.
[13] a) H. Schneider, A. Hock, R. Bertermann, U. Radius, *Chem. Eur. J.* **2017**, *23*, 12387–12398; b) H. Schneider, A. Hock, A. D. Jaeger, D. Lentz, U. Radius, *Eur. J. Inorg. Chem.* **2018**, 4031–4043; c) A. Hock, H. Schneider, M. J. Krahfuss, U. Radius, *Z. Anorg. Allg. Chem.* **2018**, *644*, 1243–1251; d) A. Hock, L. Werner, M. Riethmann, U. Radius, *Eur. J. Inorg. Chem.* **2020**, 4015–4023.
[14] N. Metzler, M. Denk, *Chem. Commun.* **1996**, 2657–2658.
[15] A. Jana, R. Azhakar, S. P. Sarish, P. P. Samuel, H. W. Roesky, C. Schulzke, D. Koley, *Eur. J. Inorg. Chem.* **2011**, 5006–5013.
[16] H. Li, F. Hung-Low, C. Krempner, *Organometallics* **2012**, *31*, 7117–7124.
[17] P. Roesch, R. Müller, A. Dallmann, G. Scholz, M. Kaupp, T. Braun, B. Braun-Cula, P. Wittwer, *Chem. Eur. J.* **2019**, *25*, 4678–4682.
[18] H. H. Karsch, P. A. Schlüter, F. Bienlein, M. Herker, E. Witt, A. Sladek, M. Heckel, *Z. Anorg. Allg. Chem.* **1998**, *624*, 295–309.
[19] For example, the bonding enthalpies for Me_3Si–Cl is 472 kJ/mol, for Me_3Sn–Cl 425 kJ/mol and for Ph_3Sn-$SnPh_3$ 189 kJ/mol, see: Y.-R. Luo, *Comprehensive Handbook of Chemical Bond Energies*, CRC Press, Boca Raton, **2007**.
[20] a) M. Saito, Y. Okamoto, M. Yoshioka, *Appl. Organomet. Chem.* **2005**, *19*, 894–897; b) T. Imori, V. Lu, H. Cai, T. D. Tilley, *J. Am. Chem. Soc.* **1995**, *117*, 9931–9940.
[21] A. F. Holleman, N. Wiberg, *Lehrbuch der Anorganischen Chemie, Vol. 102*, de Gruyter, Berlin, Deutschland, **2008**.
[22] M. K. Denk, K. Hatano, A. J. Lough, *Eur. J. Inorg. Chem.* **1998**, 1067–1070.
[23] A. Gackstatter, H. Braunschweig, T. Kupfer, C. Voigt, N. Arnold, *Chem. Eur. J.* **2016**, *22*, 16415–16419.
[24] a) D. F. Moser, T. Bosse, J. Olson, J. L. Moser, I. A. Guzei, R. West, *J. Am. Chem. Soc.* **2002**, *124*, 4186–4187; b) R. H. Walker, K. A. Miller, S. L. Scott, Z. T. Cygan, J. M. Bartolin, J. W. Kampf, M. M. Banaszak Holl, *Organometallics* **2009**, *28*, 2744–2755.
[25] a) N. Kuhn, J. Fahl, R. Boese, G. Henkel, *Z. Naturforsch. B* **1998**, *53*, 881–886; b) E. Mallah, N. Kuhn, C. Maichle-Moessmer, M. Steimann, M. Strobele, K.-P. Zeller, *Z. Naturforsch. B* **2009**, *64*, 1176–1182; c) S. Styra, M. Melaimi, C. E. Moore, A. L. Rheingold, T. Augenstein, F. Breher, G. Bertrand, *Chem. Eur. J.* **2015**, *21*, 8441–8446; d) Y. Kim, E. Lee, *Chem. Commun.* **2016**, *52*, 10922–10925; e) U. S. D. Paul, U. Radius, *Chem. Eur. J.* **2017**, *23*, 3993–4009; f) J. Emerson-King, S. A. Hauser, A. B. Chaplin, *Org. Biomol. Chem.* **2017**, *15*, 787–789; g) Z. R. Turner, *Chem. Eur. J.* **2016**, *22*, 11461–11468.
[26] a) M. Ohashi, H. Saijo, M. Shibata, S. Ogoshi, *Eur. J. Org. Chem.* **2013**, 443–447; b) M. C. Leclerc, S. I. Gorelsky, B. M. Gabidullin, I. Korobkov, R. T. Baker, *Chem. Eur. J.* **2016**, *22*, 8063–8067; c) A. J. Arduengo III, J. C. Calabrese, H. V. R. Dias, F. Davidson, J. R. Goerlich, A. Jockisch, M. Kline, W. J. Marshall, J. W. Runyon, *Phosphorus Sulfur Silicon Relat. Elem.* **2016**, *191*, 527–534.
[27] a) A. J. Arduengo III, J. C. Calabrese, F. Davidson, H. V. R. Dias, J. R. Goerlich, R. Krafczyk, W. J. Marshall, M. Tamm, R. Schmutzler, *Helv. Chim. Acta* **1999**, *82*, 2348–2364; b) A. J. Arduengo III, F. Davidson, H. V. R. Dias, J. R. Goerlich, D. Khasnis, W. J. Marshall, T. K. Prakasha, *J. Am. Chem. Soc.* **1997**, *119*, 12742–12749.
[28] a) S. Ishida, T. Iwamoto, C. Kabuto, M. Kira, *Chem. Lett.* **2001**, 1102–1103; b) S. Ishida, T. Iwamoto, C. Kabuto, M. Kira, *Silicon Chem.* **2003**, *2*, 137–140.
[29] B. Gehrhus, M. F. Lappert, *J. Organomet. Chem.* **2001**, *617–618*, 209–223.
[30] A. Jana, P. P. Samuel, G. Tavcar, H. W. Roesky, C. Schulzke, *J. Am. Chem. Soc.* **2010**, *132*, 10164–10170.
[31] V. S. V. S. N. Swamy, N. Parvin, K. Vipin Raj, K. Vanka, S. S. Sen, *Chem. Commun.* **2017**, *53*, 9850–9853.
[32] N. Wiberg, G. Ziegleder, *Chem. Ber.* **1978**, *111*, 2123–2129.
[33] A. Frenzel, J. J. Buffy, D. R. Powell, T. Müller, R. West, *Chem. Ber./Recl.* **1997**, *130*, 1579–1583.
[34] a) G. A. Miller, S. W. Lee, W. C. Trogler, *Organometallics* **1989**, *8*, 738–744; b) H.-W. Lerner, M. Bolte, N. Wiberg, *J. Organomet. Chem.* **2002**, *649*, 246–251; c) H.-W. Lerne, N. Wiberg, K. Polborn, *Z. Naturforsch. B* **2002**, *57*, 1199–1206.
[35] a) N. Wiberg, K. Schurz, G. Fischer, *Angew. Chem. Int. Ed. Engl.* **1985**, *24*, 1053–1054; *Angew. Chem.* **1985**, *97*, 1058–1059; b) N. Wiberg, K. Schurz, G. Reber, G. Müller, *J. Chem. Soc. Chem. Commun.* **1986**, 591–592.
[36] a) B. Gehrhus, P. B. Hitchcock, M. F. Lappert, *Z. Anorg. Allg. Chem.* **2001**, *627*, 1048–1054; b) L.-B. Kong, C.-M. Cui, *Organometallics* **2010**, *29*, 5738–5740; c) P. P. Samuel, R. Azhakar, R. S. Ghadwal, S. S. Sen, H. W. Roesky, M. Granitzka, J. Matussek, R. Herbst-Irmer, D. Stalke, *Inorg. Chem.* **2012**, *51*, 11049–11054; d) R. Azhakar, H. W. Roesky, J. J. Holstein, K. Pröpper, B. Dittrich, *Organometallics* **2013**, *32*, 358–361; e) Y.-L. Shan, B.-X. Leong, Y. Li, R. Ganguly, C.-W. So, *Inorg. Chem.* **2017**, *56*, 1609–1615; f) K. Yuvaraj, C. Jones, *Dalton Trans.* **2019**, *48*, 11961–11965.
[37] A. C. Tomasik, A. Mitra, R. West, *Organometallics* **2009**, *28*, 378–381.
[38] D. M. Khramov, C. W. Bielawski, *Chem. Commun.* **2005**, 4958–4960.
[39] S. Haslinger, G. Laus, V. Kahlenberg, K. Wurst, T. Bechtold, S. Vergeiner, H. Schottenberger, *Crystals* **2016**, *6*, 40/41-40/12.
[40] J. Back, J. Park, Y. Kim, H. Kang, Y. Kim, M. J. Park, K. Kim, E. Lee, *J. Am. Chem. Soc.* **2017**, *139*, 15300–15303.
[41] a) H. Quast, L. Bieber, G. Meichsner, D. Regnat, *Chem. Ber.* **1988**, *121*, 1285–1290; b) K. Peters, E. M. Peters, D. Regnat, H. Quast, *Z. Kristallogr.* **1998**, *213*, 705–706.
[42] M. Denk, R. K. Hayashi, R. West, *J. Am. Chem. Soc.* **1994**, *116*, 10813–10814.
[43] a) D. Michalik, A. Schulz, A. Villinger, *Inorg. Chem.* **2008**, *47*, 11798–11806; b) M. I. Arz, D. Hoffmann, G. Schnakenburg, A. C. Filippou, *Z. Anorg. Allg. Chem.* **2016**, *642*, 1287–1294; c) K. Bläsing, J. Bresien, R. Labbow, D. Michalik, A. Schulz, M. Thomas, A. Villinger, *Angew. Chem. Int. Ed.* **2019**, *58*, 6540–6544.
[44] P. Zark, A. Schäfer, A. Mitra, D. Haase, W. Saak, R. West, T. Müller, *J. Organomet. Chem.* **2010**, *695*, 398–408.

Manuscript received: October 8, 2020
Revised manuscript received: October 22, 2020
Accepted manuscript online: October 26, 2020